

---

# THE CAUSAL EFFECTS OF MODIFIED TREATMENT POLICIES UNDER NETWORK INTERFERENCE

---

**Salvador V. Balkus**  
Department of Biostatistics,  
Harvard T.H. Chan School of Public Health  
sbalkus@g.harvard.edu

**Scott W. Delaney**  
Department of Environmental Health,  
Harvard T.H. Chan School of Public Health  
sdelaney@mail.harvard.edu

**Nima S. Hejazi<sup>†</sup>**  
Department of Biostatistics,  
Harvard T.H. Chan School of Public Health  
nhejazi@hsph.harvard.edu

December 4, 2024

## ABSTRACT

Modified treatment policies are a widely applicable class of interventions used to study the causal effects of continuous exposures. Approaches to evaluating their causal effects assume no interference, meaning that such effects cannot be learned from data in settings where the exposure of one unit affects the outcome of others, as is common in spatial or network data. We introduce a new class of intervention—induced modified treatment policies—which we show identify such causal effects in the presence of network interference. Building on recent developments in network causal inference, we provide flexible, semi-parametric efficient estimators of the identified statistical estimand. Simulation experiments demonstrate that an induced modified treatment policy can eliminate causal (or identification) bias resulting from interference. We use the methods developed to evaluate the effect of zero-emission vehicle uptake on air pollution in California, strengthening prior evidence.

## 1 Introduction

Causal inference methodology commonly assumes *no interference*, that is, that one unit’s exposure or level does not impact any other units’ outcome (Cox, 1958; Rubin, 1980). Oftentimes, though, studies involve units that interact with one another, violating this assumption. This occurs, for instance, in settings where each study unit corresponds to a geographic area, such as a county or ZIP code area. Units often move around—as such, application of an exposure policy to a given county affects not only those residing in that region but also those commuting to and from there.

Drawing reliable conclusions about the effects of exposure policies in such settings, common as they are, necessitates the use of methodology designed to answer causal questions such as, “if one intervened upon a population via exposure  $A = a$ , how would that have changed the outcome  $Y$ ?” (Rubin, 2005). Ignoring interference between units when estimating causal effects risks invalid identification and overtly biased results (Halloran & Hudgens, 2016). Despite these challenges, data from studies that involve interference between study units can be exceedingly useful, even critical, to advancing science and policy in some settings. For instance, environmental epidemiologists may leverage observational spatial data to study the effects of pollution on human health, a case where randomized experiments are often impractical or unethical (Elliott & Wartenberg, 2004; Reich et al., 2021; Morrison et al., 2024).

However, the current state of analysis techniques in such studies fails to reliably answer questions of causality while appropriately addressing issues posed by interference. As interference frequently occurs in data generated by complex studies with a large number of variables that may confound the treatment–outcome relationship, a promising strategy is

---

<sup>†</sup> To whom correspondence should be addressed.

to use the large set of measured confounders to account for underlying interference by way of regression adjustment. Doing so requires investigators to employ *flexible* regression approaches to learn the unknown relationships while relying upon minimal assumptions that are likely to render downstream inference invalid. Compounding this issue, many studies also seek to answer questions about the effects of *continuous* (or quantitative) exposures; these pose their own challenges for identification and estimation, including possible violations of the positivity (or common support) assumption and construction of asymptotically efficient estimators. The present work aims to provide methods that can obtain inference about the causal effect of a continuous exposure while both accounting for network interference between units and using flexible regression procedures in the estimation process.

**Modified Treatment Policies** (MTPs) (Robins et al., 2004; Díaz & van der Laan, 2012; Haneuse & Rotnitzky, 2013; Young et al., 2014) are a class of interventions that define causal estimands well-suited for formulating counterfactual questions about continuous exposures. An MTP can answer the scientific question, “how much would the average value of  $Y$  have changed had the natural value of  $A$  been shifted by an increment  $\delta$ ?” (where  $\delta$  is chosen by the investigator).

Such questions are often as scientifically relevant than the analogous question answered by the causal dose-response curve—namely, “what would the average value of  $Y$  be had *every unit* been set to the same level of the treatment  $A = a$  for all  $A \in \mathcal{A}$ ?”—while being easier to pose and answer. Studies on populations exhibiting interference are frequently conducted precisely *because* considering setting every unit’s hypothetical exposure to the same level would be unrealistic in practice, making the causal dose-response curve’s assumption of common support more restrictive than necessary. The MTP framework has gained traction for its applicability in settings involving longitudinal, time-varying interventions (Díaz et al., 2023; Hoffman et al., 2024); causal mediation analysis (Díaz & Hejazi, 2020; Hejazi et al., 2023), including with time-varying mediator–confounder feedback (Gilbert et al., 2024); and causal survival analysis under competing risks (Díaz et al., 2024). However, no work has, to our knowledge, extended the MTP framework to dependent data settings characterized by interference between units.

**Contributions.** This work presents an inferential framework for estimating the causal effect of an MTP under known network interference (that is, where the interference structure is known to the investigator). First, we introduce the concept of an *induced MTP*, a new type of intervention that identifies the causal effect of an MTP when network interference is present; this is necessary to account for how the application of an MTP to a given unit affects its neighbors in the network. Next, we prove necessary and sufficient conditions for the induced MTP to yield an identifiable estimand. Then, adapting recent theoretical tools for network causal inference (Ogburn et al., 2022), we describe consistent and semi-parametric efficient estimation strategies. Finally, we evaluate how the use of an induced MTP to correct for interference can improve on classical techniques, in both numerical experiments and in a data analysis studying the effect of zero-emission vehicle uptake in California on  $\text{NO}_2$  air pollution. The tools we describe allow MTPs to be evaluated in previously intractable settings, including with spatial data and social networks.

**Outline.** Section 2 reviews MTPs and causal inference under interference. Section 3 describes the induced MTP, including identification of causal effects as well as point and variance estimation. Section 4 reports numerical results verifying the proposed methodology, while Section 5 demonstrates application in our motivating data analysis. We conclude and discuss future directions in Section 6.

## 2 Background

Throughout, we let capital bold letters denote random  $n$ -vectors; for instance,  $\mathbf{Y} = (Y_1, \dots, Y_n)$ . Consider data  $\mathbf{O} = (\mathbf{L}, \mathbf{A}, \mathbf{Y}) \sim \mathcal{P} \in \mathcal{M}$ , where  $\mathcal{P}$  is the true and unknown data-generating distribution of  $\mathbf{O}$  and  $\mathcal{M}$  is a non-parametric statistical model (i.e., set of candidate data-generating probability distributions) that places no restrictions on the data-generating distribution; in principle,  $\mathcal{M}$  may be restricted to incorporate any available real-world knowledge about the system under study. Let  $O_i = (L_i, A_i, Y_i)$  represent measurements on the  $i^{\text{th}}$  individual unit, where  $Y_i$  is an outcome of interest,  $A_i$  is a continuous exposure with support  $\mathcal{A}$ , and  $L_i$  is a collection of baseline (i.e., pre-exposure) covariates. To ease notational burden, we omit subscripts  $i$  when referring to an arbitrary unit  $i$  (i.e.,  $Y = Y_i$  when the specific unit index is not informative).

We will assume that the data-generating process can be expressed via a structural causal model (SCM, Pearl (2000)) encoding the temporal ordering between variables:  $\mathbf{L}$  is generated first, then  $\mathbf{A}$ , and finally  $\mathbf{Y}$ . We denote by  $Y(a)$  the counterfactual random variable generated by hypothetically intervening upon  $A$  to set it to  $a \in \mathcal{A}$  and observing its impact on the component of the SCM that generates  $Y$ . Our goal will be to reason scientifically about the causal relationship between  $\mathbf{A}$  and  $\mathbf{Y}$  in spite of the presence of confounders  $\mathbf{L}$  and network interference between units  $i = 1, \dots, n$ .

## 2.1 Continuous Exposures with Modified Treatment Policies

A **Modified Treatment Policy** (MTP) is a user-specified function  $d(a, l; \delta)$  that maps the observed value  $a$  of an exposure  $A$  to a new value and may itself depend on the natural (i.e., pre-intervention) value of the exposure (Haneuse & Rotnitzky, 2013).

**Example 1** (Additive Shift). For a fixed  $\delta$ , an *additive shift* MTP may be defined as

$$d(a, l; \delta) = a + \delta . \tag{1}$$

This corresponds to the scientific question, “how much of a change in  $Y$  would be caused by adding  $\delta$  to the observed natural value of  $a$ , for all units regardless of stratum  $l$ ?”

**Example 2** (Multiplicative Shift). For a fixed  $\delta$ , a *multiplicative shift* MTP is defined as

$$d(a, l; \delta) = \delta \cdot a . \tag{2}$$

This asks the scientific question “how much of a change in  $Y$  would be caused by scaling the observed natural value of  $a$  by  $\delta$ , for all units regardless of stratum  $l$ ?”

Note that in the above,  $\delta$  is a fixed, user-specified parameter specifying the magnitude of the hypothetical intervention. The MTP framework can also consider interventions that change depending on values of measured covariates  $L$ .

**Example 3** (Piecewise Additive Shift). One could propose as an MTP a piecewise additive function

$$d(a, l; \delta) = \begin{cases} a + \delta \cdot l & a \in \mathcal{A}(l) \\ a & \text{otherwise} , \end{cases} \tag{3}$$

which applies an intervention whose scale depends on the value of a covariate  $l$  and only occurs if  $a$  is within some specific subset  $\mathcal{A}(l) \subset \mathcal{A}$  of the support of  $A$ .

MTPs can be used to define scientifically relevant causal estimands for continuous exposures. The *population intervention causal effect of an MTP* (Díaz & van der Laan, 2012) is defined as  $\mathbb{E}_P(Y(d(a, l; \delta)) - Y(a))$ ; that is, the average difference between the outcome  $Y$  that did occur under the observed natural value of treatment  $a$ , i.e.,  $Y = Y(a)$ , and the counterfactual outcome  $Y(d(a, l; \delta))$  that would have occurred under the user-specified modified treatment policy  $d(a, l; \delta)$ . This estimand answers the scientific question, “what would happen if we applied some policy on the study population that modified the existing exposure according to a rule encoded by  $d(\cdot; \delta)$ ?”

MTPs are useful because they allow the investigator to specify a wide range of interpretable and realistic interventions that may be carried out in practice. In addition, MTPs may be seen as a non-parametric extension of widely used associational estimands. For example, the interpretation of the additive shift of Example 1 is a causally-informed analogue of the “risk difference” interpretation of a linear regression coefficient.

## 2.2 Causal Inference Under Interference

Interference occurs when, for a given unit  $i$ , the outcome of interest  $Y_i$  depends not only on its own assigned exposure  $A_i$  but also upon the exposure  $A_j$  of at least one other unit ( $j \neq i$ ). Formally, no interference assumes  $Y_i(a) \perp\!\!\!\perp A_j$  for all  $i \neq j$ . It is a component of the well-known stable unit treatment value assumption (SUTVA; Rubin, 1980), commonly assumed for the purpose of identification of a wide variety of causal estimands, including those defined by MTPs (Haneuse & Rotnitzky, 2013; Young et al., 2014).

Previous work has focused on settings exhibiting *partial* interference (Hudgens & Halloran, 2008; Tchetgen Tchetgen & VanderWeele, 2012; Halloran & Hudgens, 2016), which occurs when units can be partitioned into clusters such that interference only occurs between units in the same cluster. Our work focuses instead on a broader setting, that of *network interference* (van der Laan, 2014), which occurs when a unit’s outcome is subject to interference by other units’ exposures according to some arbitrary known network of relationships between units. When such interference is present, the data  $\mathbf{O}$  includes an adjacency matrix or *network profile*,  $\mathbf{F}$ , describing each units’ “friends” or neighboring units (Sofrygin & van der Laan, 2017).

Aronow & Samii (2017) demonstrate how to identify a causal estimand when SUTVA is violated due to network interference. To do this, they use an *exposure mapping*: a function that maps the exposure assignment vector  $\mathbf{A}$  to the *exposure actually received* by each unit. The exposure received is a function of a unit’s original exposure  $\mathbf{A}$  and covariates  $\mathbf{L}$ , including the network profile  $\mathbf{F}$ . If the exposure mapping is correctly specified and consistent, then SUTVA is restored and causal effects subject to interference can be identified by replacing the original exposure with that which arises from the exposure mapping. Ogburn et al. (2022) and van der Laan (2014) rely on similar logic

to identify population causal effects from data exhibiting a causally dependent structure, doing so by constructing “summary functions” of neighboring units’ exposures.

Notably, Ogburn et al. (2022) and van der Laan (2014) describe how to construct asymptotically optimal semi-parametric efficient estimators of causal effects of stochastic interventions in the network dependence setting. Stochastic interventions, which differ from MTPs, replace the natural value of exposure with a random draw from a user-specified counterfactual distribution (Díaz & van der Laan, 2012). While the hypothetical exposure that results from this random draw is not guaranteed to match that which would result from an MTP, the two classes of interventions may be constructed to yield equivalent counterfactual means (Young et al., 2014). Given the similarities between these intervention schemes, we build on previous authors’ recent theoretical developments to construct semi-parametric efficient estimators of the causal effects of MTP under network interference, thereby extending the range settings in which MTPs may be applied.

Other relevant works address interference under different assumptions: random networks (Clark & Handcock, 2024), multiple outcomes (Shin et al., 2023), long-range dependence (Tchetgen Tchetgen et al., 2021), bipartite graphs (Zigler et al., 2023), and unknown network structure (Ohnishi et al., 2022; Hoshino & Yanagi, 2023). We focus on the setting described by Ogburn et al. (2022), defined in Section 3, as their scientific goals most closely resemble those of MTPs.

### 3 Methodology

Let us first formally define the interference structure of interest. Suppose there exists a network describing whether two units are causally dependent with adjacency matrix  $\mathbf{F}$ , where  $F_i$  denotes the friends of unit  $i$ . For each unit  $i$ , a set of confounders  $L_i$  is drawn, followed by a treatment  $A_i$  based on a summary  $L_i^s$  of its own and its friends’ confounders, and finally an outcome based on  $L_i^s$  and a summary of its own and its friends’ treatment,  $A_i^s$ . This data-generating process can be defined formally as the SCM in Equation (4):

$$L_i = f_L(\varepsilon_{L_i}); A_i = f_A(L_i^s, \varepsilon_{A_i}); Y_i = f_Y(A_i^s, L_i^s, \varepsilon_{Y_i}) \quad (4)$$

Following Ogburn et al. (2022), we assume error vectors  $(\varepsilon_{L_1}, \dots, \varepsilon_{L_n})$ ,  $(\varepsilon_{A_1}, \dots, \varepsilon_{A_n})$ , and  $(\varepsilon_{Y_1}, \dots, \varepsilon_{Y_n})$  are independent of each other, with entries identically distributed and all  $\varepsilon_i \perp\!\!\!\perp \varepsilon_j$  provided  $\{i, j\} \not\subseteq F_k, \forall k \in 1, \dots, n$ ; that is, errors between units are independent provided that the units are neither directly connected nor share ties with a common node in the interference network represented by  $\mathbf{F}$ .

Interference bias arises when the data arise from the SCM (4) but investigators wrongly assume that  $f_Y$  is a function only of  $A_i$  and  $L_i$ , and not of  $\{A_j : j \in F_i\}$  or  $\{L_j : j \in F_i\}$ . Since interference violates the consistency rule (Pearl, 2010), commonly relied upon for identification of causal effects, ignoring its presence, even inadvertently, risks the drawing of unsound inferences. Under the SCM (4), identifiability of the causal effect of applying an exposure to all units  $A_j : j \in F_i$  can be restored by controlling for all  $L_j : j \in F_i$  directly or via dimension-reducing summaries (van der Laan, 2014) of a unit’s friends’ confounders and exposures.

#### 3.1 Induced Modified Treatment Policies

van der Laan (2014), Aronow & Samii (2017) and Ogburn et al. (2022) note that identifiability can be restored despite the presence of interference by basing inference on adjusting for  $A^s$  instead of  $A$  and  $L^s$  instead of  $L$ . This is, however, incompatible with the application of MTPs: we are forced to no longer consider the causal effect of  $A$  under  $d(\cdot; \delta)$ , but rather, the causal effect of  $A^s$  after intervening on the upstream exposure via  $d(\cdot; \delta)$ . To identify the causal effects of MTPs under interference, we now introduce a novel intervention scheme—the *induced MTP*.

Consider applying an MTP to the SCM (4), replacing the exposure of each unit  $A_i$  with  $A_i^* = d(A_i, L_i; \delta)$ . Under interference, we are interested in the causal effect of  $A^s$  on  $Y$ . Hence, the scientific question of interest is actually, “what if  $A_i^s$  were replaced by some  $A_i^{s,*} = h(A_i^s, L_i^s)$ ?”, where  $h$  maps the natural value of  $A_i^s$  to the value that would have resulted had  $d(\cdot; \delta)$  first been applied to  $A_i$  and only then summarized. This process is illustrated in Figure 1. We denote by  $h$  the *induced MTP*.

From Figure 1, we can see that the induced MTP  $h$  must satisfy  $(s_A \circ h)(\mathbf{A}, \mathbf{L}; \delta) = (d \circ s_A)(\mathbf{A}, \mathbf{L}; \delta)$ , where  $\circ$  denotes the function composition operator. The counterfactual mean of an induced MTP is given by Equation (5):

$$\Psi_n(\mathbf{P}) = \mathbb{E}_{\mathbf{P}} \left[ \frac{1}{n} \sum_{i=1}^n Y(h(a_i^s, l_i^s; \delta)) \right]. \quad (5)$$

This data-adaptive parameter will converge to the population counterfactual mean as  $n \rightarrow \infty$  (Hubbard et al., 2016; Ogburn et al., 2022). Use of such a parameter definition is necessary because we must condition on the single observation of the interference network at play. Under an induced MTP, interference no longer hampers identifiability

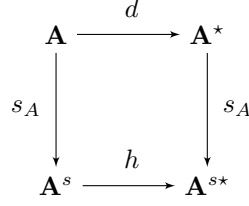


Figure 1: How an induced MTP  $h$  arises from mapping a natural summary measure  $A^s$  to the same summary after  $A$  is modified by the MTP  $d(A_i, L_i^s; \delta)$

because  $A_i^s$  captures the contribution of all relevant units (i.e., a given unit  $i$  and its friends) to each  $Y_i$ . A population intervention effect is defined by subtracting  $\mathbb{E}Y$  (Díaz & van der Laan, 2012).

### 3.2 Identification

Let  $\mathcal{A}^s$  denote the support of  $A^s$ , and  $\mathcal{L}^s$  the support of  $L^s$ . In addition to the SCM (4), identification of  $\Psi_n(P)$  by a statistical parameter  $\psi_n$  requires the following assumptions:

**A1 (Positivity).** If  $(\mathbf{a}^s, \mathbf{l}^s) \in \text{supp}\{\mathbf{A}^s, \mathbf{L}^s\}$ , then  $(h(\mathbf{a}^s, \mathbf{l}^s), \mathbf{l}^s; \delta), \mathbf{l}^s) \in \text{supp}\{\mathbf{A}^s, \mathbf{L}^s\}$

**A2 (No Unmeasured Confounding).**  $Y(a^s) \perp\!\!\!\perp A^s \mid L^s$  and  $a^s \in \mathcal{A}^s$

**A3 (Piecewise Smooth Invertibility).**  $h(a^s, l^s; \delta)$  can be written as a piecewise function over a partition  $\{A_1(l^s), \dots, A_K(l^s)\}$  of the conditional support of  $\mathcal{A}(l^s)$  of  $A^s$ , that is,

$$h(a^s, l^s) = \sum_{k=1}^K h_k(a^s, l^s; \delta) \cdot \mathbb{I}(a^s \in A_k(l^s)),$$

such that each  $h_k$  has a differentiable inverse  $h_k^{-1}$  in  $a^s$ .

With these, the counterfactual mean of an induced MTP is identified (the proof is given in Supplementary Material S1) as

$$\psi_n = \frac{1}{n} \sum_{i=1}^n \int_{\mathcal{L}^s} \int_{\mathcal{A}^s} m(a_i^s, l_i^s) w(a_i^s, l_i^s) p(a_i^s \mid l_i^s) p(l_i^s) \partial \mu(a_i^s, l_i^s), \quad (6)$$

where  $\mu$  is some dominating measure and the nuisance parameters  $m$  and  $w$  are defined as follows:

$$m(a_i^s, l_i^s) := \mathbb{E}(Y_i \mid A^s = a_i^s, L^s = l_i^s) \quad (\text{Conditional mean})$$

$$w(a_i^s, l_i^s) := \sum_{k=1}^K \frac{p(h_k^{-1}(a_i^s, l_i^s) \mid l_i^s)}{p(a_i^s \mid l_i^s)} \cdot \frac{\partial h_k^{-1}(a_i^s, l_i^s)}{\partial a_i^s} \cdot \mathbb{I}(a_i^s \in \mathcal{A}_k^s). \quad (\text{Density ratio})$$

### 3.3 Piecewise Smooth Invertibility of Induced Interventions

A key contribution of this work is outlining conditions under which piecewise smooth invertibility of  $h$  (Assumption A3) holds. Investigators generally cannot specify  $h$  directly, because doing so is unlikely to yield an intervention compatible with the network structure. Rather, investigators must start by specifying the MTP  $d(\cdot; \delta)$  and summary  $s$  to be applied to  $\mathbf{A}$ , and only then determine the function  $h$  induced by the composition  $d \circ s$ . A critical question arises: when do  $d$  and  $s$  yield a piecewise smooth invertible  $h$ ?

For brevity, we denote the vector of post-intervention exposures as  $d(\mathbf{A}) := [d(A_i, L_i; \delta)]_{i=1}^n$  and the vector of summarized exposures as  $s(\mathbf{A}) := [s_A(\{A_j : j \in F_i\}, \{L_j : j \in F_i\})]_{i=1}^n$ . Following previous definitions of summary functions for the elimination of interference (Aronow & Samii, 2017), we assume the following restrictions on  $s_A$ :

**A4 (Symmetric summaries).** Each entry in  $s$  must be a *symmetric function* in  $\{A_j : j \in F_i\}$  and in  $\{L_j : j \in F_i\}$ , that is, its values must be insensitive to permutations of its arguments' indices.

**A5 (Non-empty summaries).** Each entry in  $s$  depends on at least one entry in  $\mathbf{A}$ .

By the inverse function theorem, the derivative of the inverse of  $h$  is equal to the reciprocal of its derivative; thus, for  $h$  to be piecewise smooth invertible, it is only necessary for it to be piecewise differentiable. The following two theorems provide conditions for  $h$  to be piecewise differentiable under any  $\mathbf{F}$ :

**Theorem 1.** Under Assumptions A4 and A5, if  $h$  is to be piecewise differentiable for any  $\mathbf{F}$ , then it is necessary for  $s$  to be piecewise linear. That is, for some finite partition  $\{A_1(l^s), \dots, A_K(l^s)\}$  of the conditional support  $\mathcal{A}(l^s)$  of  $A^s$ ,  $s(\mathbf{a}) = \sum_{k=1}^K s_k(\mathbf{a})\mathbb{I}(\mathbf{a} \in A_k(l^s))$  where  $s_k(\mathbf{a})$  is a linear function and  $\mathbb{I}$  an indicator vector.

**Theorem 2.** Under Assumptions A4 and A5, for  $h$  piecewise differentiable and  $s$  any piecewise linear function,  $d$  must satisfy  $d(\mathbf{a}) = \alpha\mathbf{a} + \beta$  where  $\alpha$  is a scalar constant in  $\mathbf{a}$  and  $\beta$  is a vector such that  $\frac{\partial}{\partial \mathbf{a}}\beta = 0$ .

Taken together, Theorems 1 and 2 tell us that in order for  $h$  to be piecewise smooth invertible under *any* network structure, (1)  $s$  must be piecewise linear and (2)  $d$  can only involve a single common multiplicative shift across units, or an additive shift that may depend on covariates (or functions of  $\mathbf{a}$  with derivative zero, such as indicators). These results arise because, in general,  $s$  must be Lipschitz continuous, but, since a summary is symmetric, its Jacobian will typically be singular, requiring the Jacobian of  $d(\mathbf{a})$  to be a scalar matrix. The proofs are given in Supplementary Material S2.

The piecewise linear class of  $s$  covers a broad range of summaries, including weighted sums, order statistics, or any operation that can be interpreted as a linear combination in a vector space. Note also that Theorems 1 and 2 can be modified by restricting the forms of  $\mathbf{F}$  and  $s$ . If  $s$  is an order statistic, then  $d(\mathbf{a})$  may be any monotone function. If  $\mathbf{F}$  represents an undirected graph and the Jacobian of  $s$  is symmetric piecewise linear (for example, when  $s$  is an unweighted sum), then  $d$  may be *any* piecewise differentiable function. If  $\mathbf{F}$  represents a directed graph with no cycles, the Jacobian of  $s$  is almost surely nonsingular; if well-conditioned, the Jacobian of  $h$  in terms of  $s(\mathbf{a})$  can be obtained by Gaussian elimination. However, since  $\mathbf{F}$  and  $s$  should originate from the scientific problem at hand and cannot be chosen arbitrarily, we focus on the generic case where  $\mathbf{F}$  is arbitrary. The interested reader is invited to consult Supplementary Material S2.5 for further details.

Our identification strategy holds without restricting the form of the interference network only if  $s$  and  $d$  satisfy Theorems 1 and 2. Since asymptotically semi-parametric efficient estimators of  $\psi_n$  must be based on the appropriate efficient influence function (EIF) and thus rely on knowledge of the piecewise derivative of  $h$  (recall that it is a component of the conditional density ratio  $w(a_i^s, l_i^s)$ , necessary nuisance parameter). Theorems 1 and 2 describe when it can be computed.

### 3.4 Asymptotically Efficient Estimation

It has long since been established that plug-in or IPW-style estimators cannot leverage flexible machine learning or non-parametric regression strategies for estimation of nuisance parameters without incurring asymptotic bias (Koshevnik & Levit, 1977; Pfanzagl & Wefelmeyer, 1985; Bickel et al., 1993). Constructing a consistent estimator that achieves the semi-parametric efficiency bound—the lowest possible variance among regular asymptotically linear estimators—in the non-parametric model  $\mathcal{M}$  requires doubly-robust estimation strategies or alternative frameworks for debiased estimation.

We use *doubly robust* to mean that only the product of the rates of convergence of two nuisance estimators needs to be asymptotically negligible and for at least one nuisance estimator to be consistent for its target in order for consistent estimation of the target parameter to be achieved. Many common non-parametric regression algorithms can be shown to converge at  $n^{1/4}$  rates under conditions (see, e.g., Sec. 4.3 of Kennedy (2022) or Sec. 4.1 of Díaz et al. (2021) and references therein). As a consequence, when these algorithms are used to estimate nuisance parameters, the product of their convergence rates will generally be at least  $n^{1/2}$  (or faster), making a key second-order remainder term that appears in the relevant asymptotic expansion of the estimator and target parameter negligible; moreover, this allows for a doubly-robust estimator to achieve consistency under misspecification of either of two nuisance parameters. For the same estimator to achieve the semi-parametric efficiency bound, both nuisance parameter estimators must be correctly specified (e.g., van der Laan & Rose, 2011; Kennedy, 2022).

To construct semi-parametric efficient estimators of  $\psi_n$ , we build upon theoretical developments for estimating the causal effect of a stochastic intervention under interference. Assuming the SCM (4), Sofrygin & van der Laan (2017) showed that the causal effect of such a stochastic intervention may be identified as

$$\psi_n^* = \frac{1}{n} \sum_{i=1}^n \int_{\mathcal{L}^s} \int_{\mathcal{A}^s} m(a_i^s, l_i^s) p^*(a_i^s | l_i^s) p(l_i^s) \partial \mu(a_i^s, l_i^s), \quad (7)$$

where  $p^*$  is the mixture distribution that results from replacing each  $A_i$  with a random draw  $A_i^*$  from some user-specified distribution. Hence, the causal effect of a stochastic intervention may be viewed as measuring the average effect of replacing a random draw from  $p(a_i^s | l_i^s)$  with a random draw from  $p^*(a_i^s | l_i^s)$ .

As noted by other authors (Young et al., 2014; Díaz & van der Laan, 2018), an MTP may be expressed as a variant of a stochastic intervention whose replacement density depends on the natural value of  $A^s$  and satisfies piecewise smooth

invertibility. Here, an induced MTP is a stochastic intervention of the form

$$p^*(a_i^s | l_i^s) = \sum_{k=1}^K p(h_k^{-1}(a_i^s, l_i^s) | l_i^s) \frac{\partial h_k^{-1}(a_i^s, l_i^s)}{\partial a_i^s} \cdot \mathbb{I}(a_i^s \in \mathcal{A}_k^s). \quad (8)$$

where each  $h_k$  denotes a piece of  $h$  differentiable on domain  $\mathcal{A}_k$ .

The efficient influence function (EIF) for estimators of the statistical functional that identifies the causal effect of a stochastic intervention under interference were first derived by van der Laan (2014). Treating the EIF as an estimating equation is a standard strategy for the construction of semi-parametric efficient estimator for such functionals (Pfanzagl & Wefelmeyer, 1985; Bickel et al., 1993; van der Laan & Rose, 2011). Applying the representation in Equation (8), the EIF for the causal effect of an induced MTP is

$$\bar{\phi}_{\mathcal{P}} = \frac{1}{n} \sum_{i=1}^n w(A_i^s, L_i^s)(Y_i - m(A_i^s, L_i^s)) + \mathbb{E}_{\mathcal{P}}(m(h(A_i^s, L_i^s; \delta), L_i^s) | \mathbf{L} = \mathbf{1}) - \psi_n. \quad (9)$$

The EIF  $\bar{\phi}_{\mathcal{P}}$  is expressed as a mean because it represents the influence of all  $n$  units within the single draw of the interference network that is observed. Despite only observing a single realization of the network, it is clear to see that this EIF is composed of individual  $i$ -specific components, with the corresponding EIF estimating equation admitting the expression:

$$\bar{\phi}_{\mathcal{P}} = \frac{1}{n} \sum_{i=1}^n \phi_{\mathcal{P}}(O_i) - \psi_n = 0, \quad (10)$$

where  $\phi_{\mathcal{P}}(O_i) = w(A_i^s, L_i^s)(Y_i - m(A_i^s, L_i^s)) + \mathbb{E}_{\mathcal{P}}(m(h(A_i^s, L_i^s; \delta), L_i^s) | \mathbf{L} = \mathbf{1})$ . Ogburn et al. (2022) exploit this structure of the EIF to prove the following theorem, reproduced below for convenience:

**Theorem 3** (Central Limit Theorem of Ogburn et al. (2022):). *Suppose an estimator  $\hat{\psi}_n$  is a solution to the EIF estimating equation given in Equation (10). Also suppose that  $K_{\max}/n \rightarrow 0$  as  $n \rightarrow \infty$ , where  $K_{\max}$  denotes the maximum node degree in the network. Under the SCM (4) and mild regularity conditions,*

$$\sqrt{C_n}(\hat{\psi}_n - \psi_n^*) \xrightarrow{d} N(0, \sigma^2), \quad (11)$$

for some finite  $\sigma^2$  and some constant  $C_n$  such that  $n/K_{\max}^2 \leq C_n \leq n$ .

This theorem states that if  $K_{\max}$  grows asymptotically no faster than  $n^{1/2}$ , then an estimator  $\hat{\psi}_n$  of  $\psi_n^*$  attains a normal limiting distribution centered about  $\psi_n^*$ . In addition, these authors derive a consistent variance estimator for use in this setting; moreover, they argue, based on earlier results of van der Laan (2014), that such an estimator of  $\psi_n^*$  will exhibit rate double robustness with respect to the nuisance estimators  $\hat{m}$  and  $\hat{w}$ , with a second-order remainder term of the form  $o_{\mathcal{P}}(\sqrt{C_n}) = (\|\hat{m} - m\|_2 \|\hat{w} - w\|_2)$ , where the estimator  $\hat{\psi}_n$  of  $\psi_n^*$  remains consistent as long as the rate-product of the differences of the nuisance estimators  $\{\hat{m}, \hat{w}\}$  from their respective targets  $\{m, w\}$  converges at the specified rate. Since our target estimand  $\psi_n$  is equivalent to  $\psi_n^*$  under an MTP, using Theorem 3 and the EIF in Equation (9), we can construct semi-parametric efficient estimators of  $\psi_n$  in at least two ways, which we outline next.

**One-Step Estimation.** A one-step estimator (Pfanzagl & Wefelmeyer, 1985; Bickel et al., 1993) uses Equation (10) to de-bias an initial plug-in estimator of  $\psi_n$  by adding to it an estimated  $\phi_{\hat{\mathcal{P}}_n}(O_i)$  based on nuisance estimators.

Note that  $P_n$  denotes the empirical distribution, while  $\hat{P}_n$  denotes the empirical distribution augmented by nuisance estimates. The outer expectation in the term  $\mathbb{E}_{\mathcal{P}}(\hat{m}(h(A_i^s, L_i^s; \delta), L_i^s) | \mathbf{L} = \mathbf{1})$  in the EIF can be dropped because the sample means of  $\hat{m}(h(A_i^s, L_i^s; \delta), L_i^s)$  and  $\mathbb{E}_{\mathcal{P}}(\hat{m}(h(A_i^s, L_i^s; \delta), L_i^s) | \mathbf{L} = \mathbf{1})$  both converge to the same value (see Supplementary Materials S3 for a proof). Then, the one-step estimator is

$$\hat{\psi}_n^{\text{OS}} = \frac{1}{n} \sum_{i=1}^n \phi_{\hat{\mathcal{P}}_n}(O_i), \quad (12)$$

where  $\phi_{\hat{\mathcal{P}}_n}(O_i) = \hat{w}(A_i^s, L_i^s)(Y_i - \hat{m}(a_i^s, l_i^s)) + \hat{m}(h(A_i^s, L_i^s; \delta), L_i^s)$ . Since the estimating functions are no longer centered, variance estimates must be adjusted (as described in Section 3.6). The one-step estimator achieves the semi-parametric efficiency bound, the asymptotic limiting variance of the class of regular asymptotically linear estimators in the non-parametric model  $\mathcal{M}$ .

**Targeted Maximum Likelihood Estimation (TMLE).** Although the one-step estimator is semi-parametric efficient, it is not a substitution estimator; it may yield parameter estimates outside the bounds of the parameter space. TMLE resolves this shortcoming; it is a general template for the construction of substitution estimators that appropriately solve the EIF estimating equation (van der Laan & Rubin, 2006; van der Laan & Rose, 2011). Estimation under an MTP proceeds as follows:

1. Estimate nuisance functions to obtain  $\hat{w}(A_i^s, L_i^s)$ ,  $\hat{m}(A_i^s, L_i^s)$ , and  $\hat{m}(h(A_i^s, L_i^s, \delta), L_i^s)$ .
2. Fit a one-dimensional parametric model regressing  $\hat{w}(A_i^s, L_i^s)$  on  $Y_i$  with offset  $\hat{m}(A_i^s, L_i^s)$ ; a common choice is the logistic regression  $\text{logit}(Y_i) = \text{logit}(\hat{m}(A_i^s, L_i^s)) + \varepsilon \hat{w}(A_i^s, L_i^s)$ , where the  $Y_i$  are rescaled to ensure each lies in the interval  $(0, 1)$ .
3. Compute  $\hat{m}^*(h(A_i^s, L_i^s; \delta), L_i^s) = \text{expit}(\text{logit}(\hat{m}(h(A_i^s, L_i^s; \delta), L_i^s)) + \hat{\varepsilon} \hat{w}_n(h(A_i^s, L_i^s; \delta), L_i^s))$ , the parametric model predictions.
4. Compute the TML estimate as  $\psi_n^{\text{TMLE}} = \frac{1}{n} \sum_{i=1}^n \hat{m}^*(h(A_i^s, L_i^s; \delta), L_i^s)$ .

In Step 2, the corresponding estimate  $\hat{\varepsilon}$  is used to fluctuate the initial estimator  $\hat{m}(A_i^s, L_i^s)$ , using the density ratio  $w(A_i^s, L_i^s)$ , to an updated version  $\hat{m}^*(A_i^s, L_i^s)$  in such a way that the EIF estimating equation is solved. Logistic regression is commonly employed to guarantee each prediction  $\hat{m}^*$  falls in the bounds of the parameter space, thus respecting global constraints (Gruber & van der Laan, 2010). One can also fit an intercept-only model with  $\hat{w}$  as weights, which may improve stability. In what follows, we refer to this estimator as “network-TMLE,” following Zivich et al. (2022), who discuss its use in practical settings and examine its properties in simulation experiments.

### 3.5 Nuisance Parameter Estimation

The underlying form of nuisance parameters  $m$  and  $w$  is usually recognized to be unknown and may involve, for example, complex nonlinear interactions between covariates. Therefore, it is desirable to estimate such quantities using modeling approaches that are flexible. In this process,  $K$ -fold cross-fitting can be employed to ensure that the training data used to construct nuisance estimators are independent of the nuisance predictions used in the final estimation procedure (Zheng & Van Der Laan, 2010; Chernozhukov et al., 2018); it has long been recognized that this form of sample-splitting can eliminate the need for empirical process conditions (Pfanzagl & Wefelmeyer, 1985; Klaassen, 1987), though extensions of such conditions to the network interference setting discussed in a recent study (Bong et al., 2024). Importantly, note that in the presentation above, we have, for convenience and clarity, suppressed notation for such sample-splitting.

Since the *outcome regression*  $m$  is a conditional expectation function, it can be estimated using any supervised learning algorithm. We recommend super learning (van der Laan et al., 2007), that is, fitting an ensemble of regression models in a cross-validated manner and selecting the model yielding the lowest cross-validated risk (for continuous outcomes, we use mean-squared error). This guarantees that the selected regression model performs asymptotically as well as the best candidate predictor in the library used to construct the ensemble (van der Laan et al., 2004; van der Vaart et al., 2006), even in the fixed regression design setting presently considered (Davies & van der Laan, 2016). Phillips et al. (2023) proposed guidance and heuristics to aid in overcoming the considerable challenge of assembling a candidate library from the diversity of learning algorithms available.

An advantage of the MTP framework is that the implied form of the intervention, unlike general stochastic interventions (Díaz & van der Laan, 2012; Sofrygin & van der Laan, 2017; Ogburn et al., 2022), facilitates direct estimation of the density ratio  $w$ , circumventing the need to fit a conditional density. A common density ratio estimator is based on probabilistic classification (Qin, 1998; Cheng & Chu, 2004), in which a classifier is trained to distinguish between natural and intervened samples, and its output is transformed into a density ratio using Bayes’ rule. The use of this method with an MTP is described in detail by Díaz et al. (2023, see Section 5.4). We recommend super learning with binary log loss to select the optimal classifier. One can also employ kernel-based methods, including Kernel Mean Matching, Kullback-Leibler Importance Estimation, and Least-Squares Importance Fitting, as outlined in detail by Sugiyama et al. (2012).

### 3.6 Variance Estimation

Summary measures are correlated if they aggregate common units. As a result, the as-iid sample variance of the estimated EIF will be conservative, especially if the network degree distribution is highly skewed (Sofrygin & van der Laan, 2017). Ogburn et al. (2022) show that a consistent variance estimator for the solution to an arbitrary estimating equation  $\frac{1}{n} \sum_{i=1}^n \varphi_i = 0$  with some arbitrary estimating function  $\varphi_i$  satisfying  $\mathbb{E}(\varphi_i) = 0$  is given by

$$\hat{\sigma}^2 = \frac{1}{n^2} \sum_{i,j} G(i,j) \varphi_i \varphi_j, \quad (13)$$

where  $G(i,j) = 1$  if  $i = j$ ,  $i$  and  $j$  are in each others’ dependency neighborhoods, or  $i$  and  $j$  share a friend  $k$ , and  $G(i,j) = 0$  otherwise.

As the estimators from Section 3.4 are constructed based on the *uncentered* estimating function  $\phi_P(O_i)$ , this result does not transport directly to our setting. However, examining the SCM (4) reveals that  $O_i$  and  $O_j$  will be identically distributed and therefore have the same mean provided that they have the same number of neighbors (that is,  $|F_i| = |F_j|$ ). Following a similar strategy as Emmenegger et al. (2023), a centered estimating function is  $\phi_P(O_i) - \psi_n(|F(O_i)|)$ , where  $\psi_n(|F(O_i)|)$  denotes the mean of  $\phi_P(O_j)$  over all units in  $j \in 1, \dots, n$  satisfying the equality  $|F_j| = |F_i|$ . This centering term can be estimated by computing  $\hat{\psi}_n^{\text{OS}}$  within each sub-group of possible  $|F_i|$  values. Let  $\mathcal{N}(m) = \{k : k \in 1, \dots, n, |F_k| = m\}$ . Formally, this is

$$\hat{\psi}_n(|F_i|) = \frac{1}{|\mathcal{N}(|F_i|)|} \sum_{j \in \mathcal{N}(|F_i|)} \phi_{\hat{P}_n}(O_j) \quad (14)$$

Then, letting  $\varphi_i = \phi_{\hat{P}_n}(O_i) - \hat{\psi}_n(|F_i|)$ , the variance estimator  $\hat{\sigma}^2$  as described in Equation (13) is a consistent estimator of the variance of  $\hat{\sigma}_n^{\text{OS}}$  and  $\hat{\sigma}_n^{\text{TMLE}}$ , provided both nuisance estimators are consistent for their targets (See proof in Supplementary Material, Section S4).

## 4 Results: Numerical Simulations

We now empirically evaluate the performance of the estimators described in Section 3. All data in this section are simulated in the numerical computing language Julia (Bezanson et al., 2017), using the package `CausalTables.jl` (Balkus & Hejazi, 2024a). MTP estimates are computed using `ModifiedTreatment.jl` (Balkus & Hejazi, 2024b), a Julia package implementing the estimators described in this work. Unless otherwise specified, conditional mean and density ratio nuisance parameters are estimated using super learning (van der Laan et al., 2007) to select the candidate algorithm—from an ensemble consisting of a GLM, random forest, and multiple gradient boosted tree models with various sets of hyperparameters—that minimizes the cross-validated empirical risk with respect to an appropriate loss function (MSE for the conditional mean, binary log-loss for the density ratio). Code for these experiments and the following data analysis is available on GitHub at <https://github.com/salbalkus/pub-code-mtp-interfere>.

### 4.1 Synthetic Data Results

First, we evaluate estimators on simulated data with both network interference and nonlinear relationships between confounders, exposure, and outcome. We simulate this data using three common network structures: Erdős-Rényi (with  $p = 4/n$ ), static scale-free (with  $\lambda = 3.5$ ), and Watts-Strogatz (with  $K = 4$  and  $\beta = 0.5$ ). Data are generated according to the following set of structural equations:

$$\begin{aligned} \mathbf{L}_1 &\sim \text{Beta}(3, 2); \mathbf{L}_2 \sim \text{Poisson}(100); \mathbf{L}_3 \sim \text{Gamma}(2, 4); \mathbf{L}_4 \sim \text{Bernoulli}(0.6) \\ \mathbf{A} &\sim \text{Normal}(0.1m_L, 1.0) \text{ and } \mathbf{A}^s = \left[ \sum_{j \in F_i} A_j \right]_{i=1}^n \\ \mathbf{Y} &\sim \text{Normal}(0.2\mathbf{A} + \mathbf{A}^s + 0.2m_L, 0.1), \end{aligned} \quad (15)$$

where  $m_L = (L_2 > 50) + (L_2 > 100) + (L_2 > 200) + (L_3 > 0.1) + (L_3 > 0.5) + (L_3 > 4) + (L_3 > 10) + L_4 + L_4 \cdot \left( (L_1 > 0.4) + (L_1 > 0.6) + (L_1 + 0.8) \right)$ . We estimate the counterfactual mean under the MTP  $d(a, l) = a + 0.2$ , comparing network-TMLE which accounts for interference using the induced MTP to standard linear regression and IID-TMLE, which do not account for interference; results using the one-step estimator were nearly identical and therefore omitted for brevity.

Figure 2 demonstrates how the empirical performance of our estimator using network-TMLE aligns with theoretical results outlined in Section 3. Bias reliably converges to zero with increasing sample size across all three network structures. As computing the scaling factor  $\sqrt{C_n}$  for the semi-parametric efficiency bound is currently intractable, we remark that the  $n^{1/2}$ -scaled bias and  $n$ -scaled MSE stay roughly constant. This indicates both that the TMLE estimator converges at a reasonable rate (compared to  $n^{1/2}$ ) and that its MSE is bounded. In addition, the coverage rate of the 95% confidence interval converges to the nominal level. Hence, the estimator performs as expected. This demonstrates how accounting for interference can yield drastic improvements in estimator performance. Across all metrics, network-TMLE outperforms both standard linear regression, which suffers from lack of model flexibility and failure to account for interference, and IID-TMLE, which is flexible but also ignores interference. As a result, their bias does not dissipate asymptotically, and 95% confidence intervals achieve close to zero coverage.

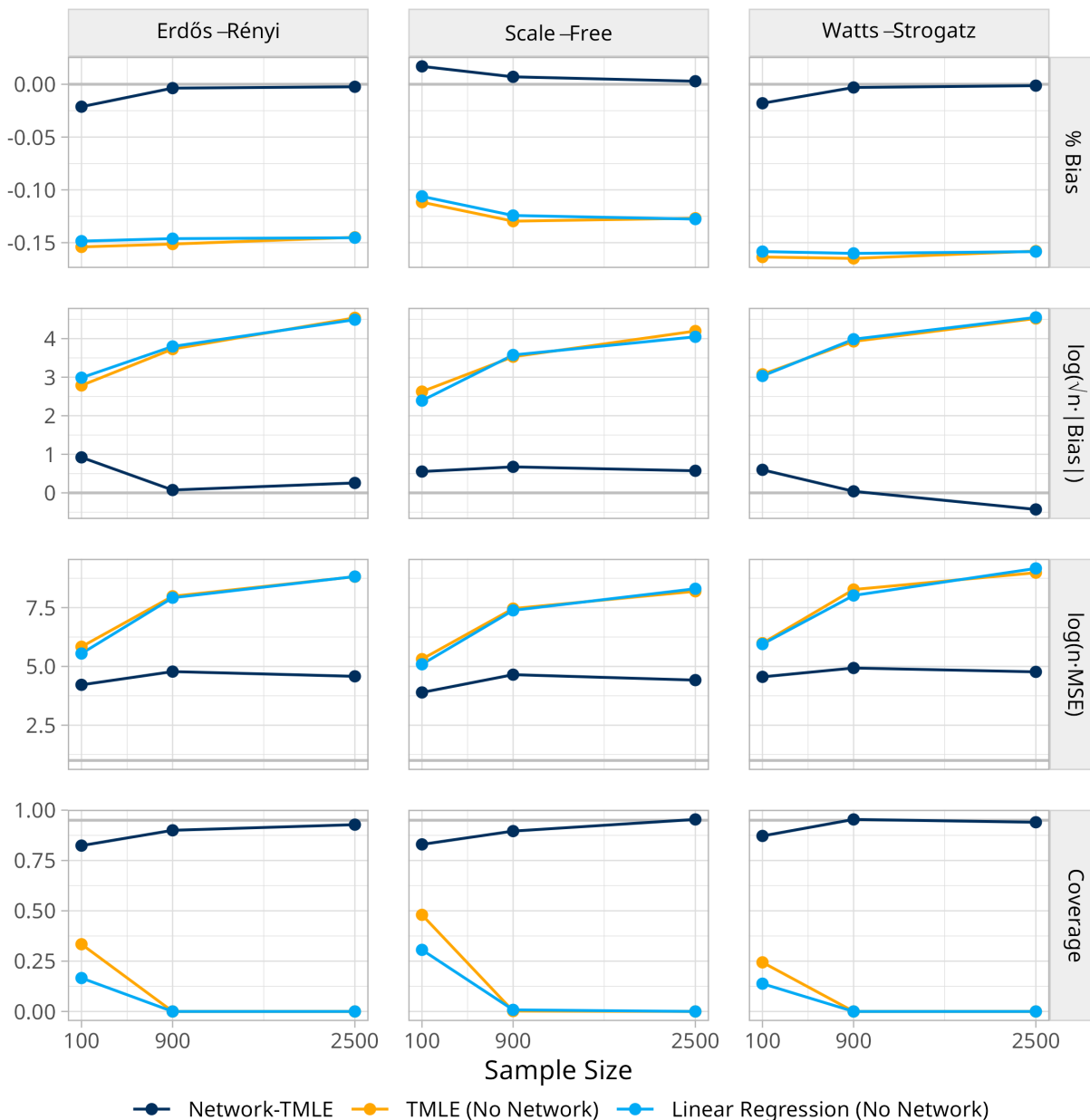


Figure 2: Performance of network-TMLE compared to other common models on MTP estimation with various types of network profiles. Results jittered for visibility.

## 4.2 Semi-Synthetic Data Results

In a second simulation experiment, we generate semi-synthetic data based on the real-world dataset that inspired this work and that is analyzed in Section 5. Sixteen confounding variables are taken as fixed covariates, with the 2013 and 2019 LODES commuting pattern data (U.S. Census Bureau, 2024) for California as the network profile. From these, we draw exposure and outcome distributions from a normal distribution with mean following a linear function of the confounders and  $A_s$ , a trimmed sum of neighbors' values of  $A$  over friends that contributed at least 5% of commuters

into the given unit. These are represented by structural equations, conditional on  $\mathbf{L}$  and  $\mathbf{F}$ , expressed as

$$\begin{aligned} \mathbf{A} &\sim \text{Normal}(0.01 \cdot \mathbf{L}\beta, 1.0) \text{ and } \mathbf{A}^s = \left[ \sum_{j \in F_i} A_j \right]_{i=1}^n \\ \mathbf{Y} &\sim \text{Normal}(\mathbf{A} + \mathbf{A}^s + 0.1 \cdot \mathbf{L}\beta, 1.0), \end{aligned} \tag{16}$$

where  $\beta$  is a constant vector chosen to ensure no single confounder overly influenced the resulting outcome.

We estimate the population causal effect of an MTP in 500 simulations using four different estimators: network-TMLE with correctly-specified GLMs (linear regression for the outcome regression and logistic regression for the density ratio probabilistic classifier), network-TMLE with super learning for both nuisance estimators, IID-TMLE with correctly-specified GLMs, and main-terms linear regression. In this simulation,  $n = 1652$ , the same as in the empirical dataset considered in Section 5.

Table 1 depicts the percent bias, coverage of 95% confidence intervals (using covariate-conditional variance estimates), and MSE of the estimators. It is again clear from inspection that accounting for network interference can yield dramatically lower bias, even when the outcome regression model is otherwise correctly specified. In this case, using network-TMLE with a correctly specified GLM decreased the mean percent bias from over 100% (estimates double the true value) to about 0.5%, and cut MSE by about three-fourths compared to a standard main-terms linear regression. Even if super learning is used, the mean percent bias of the network-TMLE remains relatively low, at around 6.6%, and the MSE is approximately identical. Furthermore, confidence interval coverage for the network-TMLE is close to nominal under both nuisance estimators. Alternative methods suffer greatly reduced coverage due to their severe bias.

Table 1: Network-TMLE on semi-synthetic data vs. competing estimators

Method	Learner	Bias (%)	Coverage (%)	MSE
Network-TMLE	Correct GLM	0.45	95.2	0.013
	Super Learner	-6.58	95.0	0.013
IID-TMLE	Correct GLM	-103.39	26.0	0.049
Linear Regression		-103.52	54.2	0.057

Since super learning of nuisance estimates yields relatively low bias and MSE, we use the same super learner library in the next section. As this simulation relied on the same covariates and network structure as our illustrative data analysis, we expect our approach to perform reasonably well in the Section 5 data analysis.

## 5 Data Application: Mobile Source Air Pollution

In this section, we use induced MTPs to analyze the causal effect of “zero-emissions” vehicle (ZEV) uptake in California on  $\text{NO}_2$  air pollution using observational data.  $\text{NO}_2$  is a byproduct of gasoline-powered vehicles shown to be associated with adverse health outcomes, including respiratory issues and mortality (Hesterberg et al., 2009; Gillespie-Bennett et al., 2010; Faustini et al., 2014). In the U.S., national ambient air quality standards (NAAQs) are set by the Environmental Protection Agency that limit the amount of allowable  $\text{NO}_2$  in the air (United States EPA, 2018).

As ZEVs do not produce tailpipe emissions, including  $\text{NO}_2$ , governments have heavily promoted their adoption to limit air pollution. State governments must ascertain whether these policies work as intended; hence, understanding how much localized air pollution has decreased as a result of increased ZEV adoption is of both scientific and policy interest. Garcia et al. (2023) analyzed whether ZEV uptake was associated with  $\text{NO}_2$  air pollution across zip code tabulation areas (ZCTA) in California from 2013 to 2019. They found that an increase of 20 ZEVs per 1000 population was associated with a reduction of 0.41 parts-per-billion in  $\text{NO}_2$  within a given ZCTA on average; however, with a  $p$ -value of 0.252 and confidence interval of  $(-1.12, 0.29)$ , this finding was not statistically significant.

This is a problem in which network interference arises as a result of people driving outside of the ZCTA in which they reside; that is, they commute in their vehicles to other ZCTAs, emitting pollution there as well. Garcia et al. (2023) controlled for confounding using a linear model, without accounting for interference from people commuting in vehicles from one ZCTA unit to another. As evidenced by our simulations in Section 4, neglecting interference can yield bias and misleading confidence intervals. In addition, overreliance on linear modeling may be cause for

concern, as linearity imposes a strict functional form which may be incorrect, also resulting in bias. The goal of our data analysis is to study the same research question as Garcia et al. (2023) and compare how flexibly modeling the causal effect of an induced MTP can improve inference in this setting.

Following Garcia et al. (2023), we compute the exposure, the percentage of light-duty vehicles in California actively registered as ZEVs by April 2019, for each ZCTA from the California Energy Commission (2024). The outcome, change in  $\text{NO}_2$  from 2013 to 2019 in parts per billion (ppb), is spatially aggregated from a 1 km grid of estimated pollution levels (Cooper, 2022a,b); this provides finer-grain ZCTA-level estimates than the raw sensor data used by Garcia et al. (2023). Socioeconomic confounders are accessed from the U.S. Census via Walker & Herman (2024), while land-use confounders are obtained from U.S. Environmental Protection Agency (2024). See Supplementary Material S5 for summary statistics. We performed spatial alignment and areal weighted interpolation of missing values using the `sf` (Pebesma, 2018) and `areal` (Prener et al., 2019) packages in the statistical computing language R (R Core Team, 2024).

Finally, to account for interference, we rely on a commuting network describing the number of people traveling between home and work ZCTAs (de Souza et al., 2023; U.S. Census Bureau, 2024). The induced MTP summary function is an estimate of the percentage of incoming work commuters driving ZEVs during the same period. This was computed by summing the percentage of ZEVs in each neighboring ZCTA in the network, with each summand weighted by the percentage of each neighbor’s population who drive to work, and then normalized to convert back into a percentage. Sums of neighboring covariates are also included as potential confounders for the induced MTP.

We compared the following data-analytic strategies: (1) estimating an induced MTP using network-TMLE, (2) estimating a classical MTP using TMLE, and (3) estimating main-terms GLM regression coefficients. Each answers the same question: “how much *more* would  $\text{NO}_2$  have decreased from 2013 to 2019 on average had each ZCTA experienced an increase in the percentage of vehicles registered as ZEV in California by 2019?” Strategy (1) accounts for interference and fits nuisance parameters using flexible super learning. Strategy (2) also uses super learning, but ignores interference. Strategy (3) imposes a strict assumption of linearity and also ignores interference.

## 5.1 Results

Figure 3 displays effect estimates of increasing the percentage of ZEVs in each ZCTA by one percent – the additive shift from Example 1 – as well as scaling the percentage of ZEVs up by 20%, the multiplicative shift from Example 2. According to the induced MTP effect estimate, adding 1 percent to the proportion of ZEVs across ZCTAs would yield a 0.042 ppb decrease in  $\text{NO}_2$  on average. This estimate is over 30% larger than the MTP effect estimate not accounting for interference (0.032 ppb), and about 2.8 times larger than the GLM-based estimate (0.015 ppb). Similarly, the induced MTP effect estimate indicated that scaling the proportion of ZEVs by 20% across ZCTAs would yield a 0.046 ppb decrease in  $\text{NO}_2$  on average – over 40% larger than the interference-ignoring MTP effect estimate (0.032 ppb) and the GLM-based estimate (0.027 ppb).

Accounting for interference and using flexible regression and machine learning yielded even larger effect estimates than those typically recovered by prior analyses, suggesting commuting contributes significantly to  $\text{NO}_2$  air pollution. This was especially pronounced for the multiplicative shift, possibly demonstrating that vehicular  $\text{NO}_2$  is driven significantly by ZCTAs with large numbers of out-commuters. The proposed procedure also yielded estimates with lower variance.

Figure 4 displays effect estimates over a grid of possible additive and multiplicative shifts. At low-magnitude shifts, the estimates were roughly the same. However, at larger shifts—about 0.75% on the additive scale and 10% on the multiplicative scale—the estimated effects diverged, with effects accounting for interference becoming more pronounced. The trend in estimated effect was also less erratic under the multiplicative shift. This may be because the multiplicative shift only produces a large shift among ZCTAs with a large proportion of ZEVs, avoiding empirical positivity issues that may destabilize the estimators. Such a result highlights the importance of only considering MTPs that can be easily estimated from the data available.

## 6 Discussion

In this work, we introduced the induced modified treatment policy, a new class of MTP that accounts for known network interference. This intervention is useful for causal inference in observational data settings that feature continuous exposures and network interference. We proved that in order for the causal effect of an induced MTP to be identified under arbitrary network interference and estimated using semi-parametric efficiency theory, the summary of the exposure must be piecewise linear.

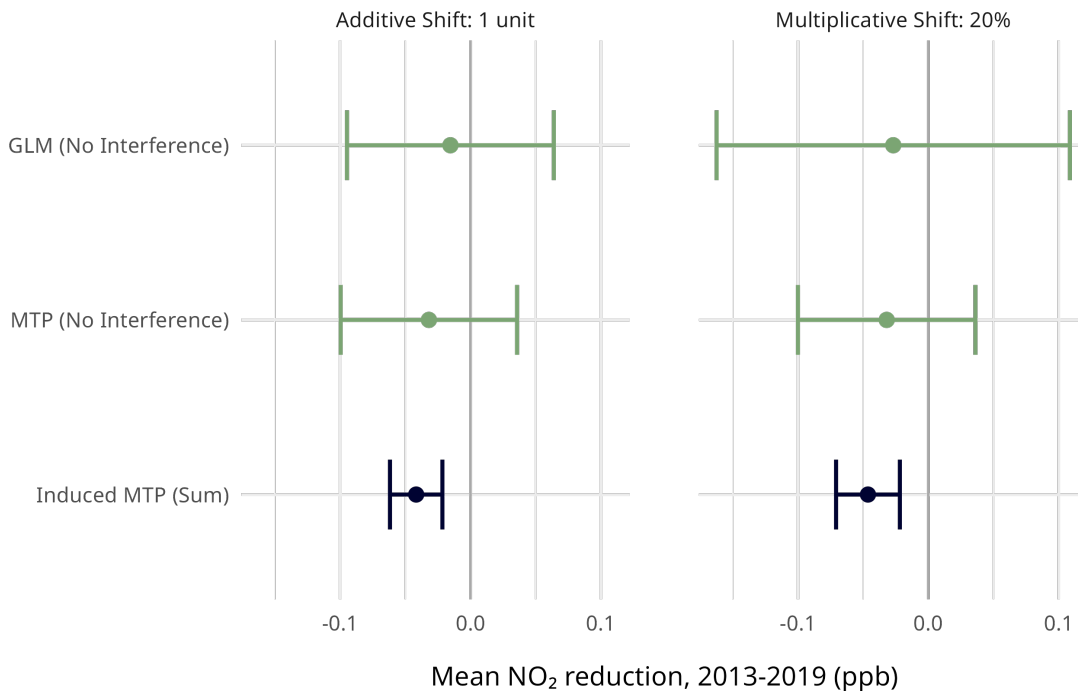


Figure 3: Estimated effect sizes measuring the expected difference in  $\text{NO}_2$  across California ZCTAs caused by two different increases in the proportion of ZEVs in 2019.

Using simulation experiments on synthetic and semi-synthetic data, we showed that interference can result in significant bias when it is not corrected for using an induced MTP. Our illustrative data analysis demonstrates the perils of ignoring interference and applying restrictive linear modeling-based strategies in settings with observational spatial data, as is often used in fields like environmental epidemiology; such oversimplifications can yield vastly different conclusions than those provided by our proposed estimation strategy. Estimating an induced MTP using network-TMLE yields increased precision and unbiased results in the presence of known network interference.

In practice, several challenges remain. One limitation is that ratios of conditional densities are still more difficult to estimate than conditional expectation functions, especially in high-dimensional settings (Sugiyama et al., 2012). This is even more problematic under interference: for units with an excessively large number of neighbors, the density ratio between the natural and post-intervention exposure could grow extremely large, compromising downstream estimates.

In addition, practitioners must know how the interference arises. This does often occur; in our data analysis, the form of interference arose naturally as a part of the scientific question that considered an intervention on *all* vehicles entering a given ZCTA, not just those registered there. If an investigator has reason to suspect interference, they may also suspect the underlying process by which it occurs. However, there are cases where an investigator may not know the form. Although discussed in recent work (Hoshino & Yanagi, 2023; Ohnishi et al., 2022), this remains an avenue for future research.

Other potential areas of future research involve extending the induced MTP to more difficult causal inference problems. In the time-varying setting, for example, one might consider using an induced *longitudinal* MTP (Díaz et al., 2023), which would require involved sequential regression-based algorithms for to account for summary measures of exposures involving a network profile that evolves across time steps. Further work overcoming the technical limitations of estimating the effects of induced MTPs will be critical to facilitate answering more complex causal inference questions. This will be important for obtaining better scientific insights in settings where continuous exposures are measured within datasets exhibiting network interference.

## Acknowledgments

SVB was supported in part by grants from the National Institute of Environmental Health Sciences (award no. T32 ES007142) and the National Science Foundation (award no. DGE 2140743). The authors thank Rachel Nethery for her help in initiating the motivating data analysis.

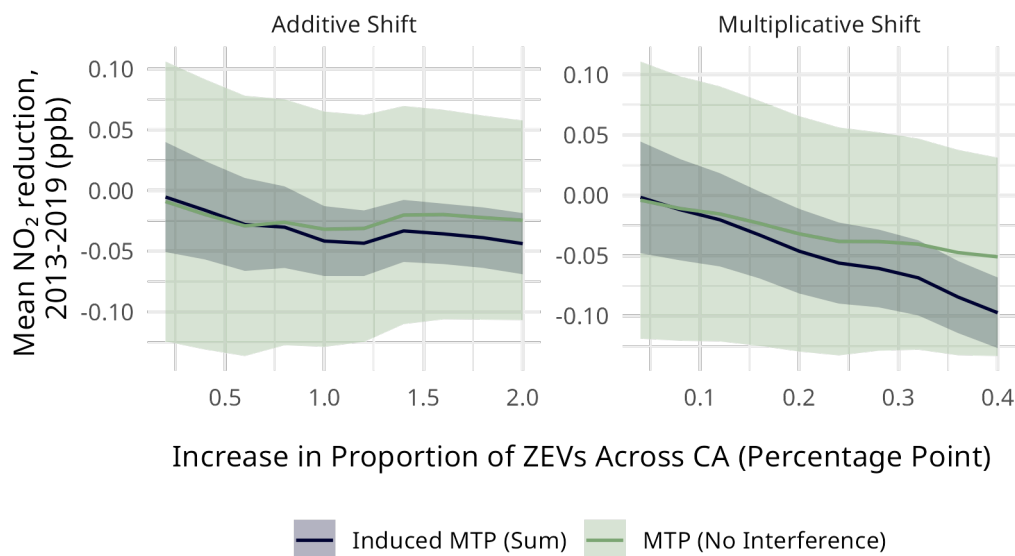


Figure 4: Estimated effect sizes measuring the expected difference in NO<sub>2</sub> across California ZCTAs caused by various additive or multiplicative shifts in the percentage of ZEVs in 2019. Confidence bands are based on a Bonferroni correction.

*Conflicts of interest:* The authors have no conflicts of interest to disclose.

## References

- ARONOW, P. M. & SAMII, C. (2017). Estimating average causal effects under general interference, with application to a social network experiment. *The Annals of Applied Statistics* **11**, 1912–1947.
- BALKUS, S. & HEJAZI, N. (2024a). `CausalTables.jl`. <https://github.com/salbalkus/CausalTables.jl>.
- BALKUS, S. & HEJAZI, N. (2024b). `ModifiedTreatment.jl`. <https://github.com/salbalkus/ModifiedTreatment.jl>.
- BEZANSON, J., EDELMAN, A., KARPINSKI, S. & SHAH, V. B. (2017). Julia: A fresh approach to numerical computing. *SIAM Review* **59**, 65–98.
- BICKEL, P. J., KLAASSEN, C. A., BICKEL, P. J., RITOV, Y., KLAASSEN, J., WELLNER, J. A. & RITOV, Y. (1993). *Efficient and adaptive estimation for semiparametric models*, vol. 4. Springer.
- BONG, H., FOGARTY, C. B., LEVINA, L. & ZHU, J. (2024). Unraveling heterogeneous treatment effects in networks: A non-parametric approach based on node connectivity. *arXiv:2410.11797*.
- CALIFORNIA ENERGY COMMISSION (2024). Light-duty vehicle population in california .
- CHENG, K. & CHU, C. (2004). Semiparametric density estimation under a two-sample density ratio model. *Bernoulli* **10**.
- CHERNOZHUKOV, V., CHETVERIKOV, D., DEMIRER, M., DUFLO, E., HANSEN, C., NEWEY, W. & ROBINS, J. (2018). Double/debiased machine learning for treatment and structural parameters. *The Econometrics Journal* **21**, C1–C68.
- CLARK, D. A. & HANDCOCK, M. S. (2024). Causal inference over stochastic networks. *Journal of the Royal Statistical Society Series A: Statistics in Society* **187**, 772–795.
- COOPER, M. (2022a). Satellite-derived ground level no2 concentrations, 2005-2019.
- COOPER, M. (2022b). Tropomi-derived ground level no2 concentrations (2019 annual mean).
- COX, D. R. (1958). Planning of experiments. .
- DAVIES, M. M. & VAN DER LAAN, M. J. (2016). Optimal spatial prediction using ensemble machine learning. *The International Journal of Biostatistics* **12**, 179–201.

- DE SOUZA, P., ANENBERG, S., MAKAREWICZ, C., SHIRGAOKAR, M., DUARTE, F., RATTI, C., DURANT, J. L., KINNEY, P. L. & NIEMEIER, D. (2023). Quantifying disparities in air pollution exposures across the United States using home and work addresses. *Environmental Science & Technology* **58**, 280–290.
- DÍAZ, I. & HEJAZI, N. S. (2020). Causal mediation analysis for stochastic interventions. *Journal of the Royal Statistical Society: Series B (Statistical Methodology)* **82**, 661–683.
- DÍAZ, I., HEJAZI, N. S., RUDOLPH, K. E. & VAN DER LAAN, M. J. (2021). Non-parametric efficient causal mediation with intermediate confounders. *Biometrika* **108**, 627–641.
- DÍAZ, I., HOFFMAN, K. L. & HEJAZI, N. S. (2024). Causal survival analysis under competing risks using longitudinal modified treatment policies. *Lifetime Data Analysis* **30**, 213–236.
- DÍAZ, I. & VAN DER LAAN, M. (2012). Population intervention causal effects based on stochastic interventions. *Biometrics* **68**, 541–549.
- DÍAZ, I. & VAN DER LAAN, M. J. (2018). Stochastic treatment regimes. In *Targeted Learning in Data Science: Causal Inference for Complex Longitudinal Studies*. Springer Science & Business Media, pp. 167–180.
- DÍAZ, I., WILLIAMS, N., HOFFMAN, K. L. & SCHENCK, E. J. (2023). Nonparametric causal effects based on longitudinal modified treatment policies. *Journal of the American Statistical Association* **118**, 846–857.
- ELLIOTT, P. & WARTENBERG, D. (2004). Spatial epidemiology: Current approaches and future challenges. *Environmental Health Perspectives* **112**, 998–1006.
- EMMENEGGER, C., SPOHN, M.-L., ELMER, T. & BÜHLMANN, P. (2023). Treatment effect estimation with observational network data using machine learning. *arXiv:2206.14591*.
- FAUSTINI, A., RAPP, R. & FORASTIERE, F. (2014). Nitrogen dioxide and mortality: review and meta-analysis of long-term studies. *European Respiratory Journal* **44**, 744–753.
- GARCIA, E., JOHNSTON, J., MCCONNELL, R., PALINKAS, L. & ECKEL, S. P. (2023). California’s early transition to electric vehicles: Observed health and air quality co-benefits. *Science of The Total Environment*, 161761.
- GILBERT, B., HOFFMAN, K. L., WILLIAMS, N., RUDOLPH, K. E., SCHENCK, E. J. & DÍAZ, I. (2024). Identification and estimation of mediational effects of longitudinal modified treatment policies. *arXiv:2403.09928*.
- GILLESPIE-BENNETT, J., PIERSE, N., WICKENS, K., CRANE, J. & HOWDEN-CHAPMAN, P. (2010). The respiratory health effects of nitrogen dioxide in children with asthma. *European Respiratory Journal* **38**, 303–309.
- GRUBER, S. & VAN DER LAAN, M. J. (2010). A targeted maximum likelihood estimator of a causal effect on a bounded continuous outcome. *The International Journal of Biostatistics* **6**.
- HALLORAN, M. E. & HUDGENS, M. G. (2016). Dependent happenings: A recent methodological review. *Current Epidemiology Reports* **3**, 297–305.
- HANEUSE, S. & ROTNITZKY, A. (2013). Estimation of the effect of interventions that modify the received treatment. *Statistics in Medicine* **32**, 5260–5277.
- HEJAZI, N. S., RUDOLPH, K. E., VAN DER LAAN, M. J. & DÍAZ, I. (2023). Nonparametric causal mediation analysis for stochastic interventional (in)direct effects. *Biostatistics* **24**, 686–707.
- HESTERBERG, T. W., BUNN, W. B., MCCLELLAN, R. O., HAMADE, A. K., LONG, C. M. & VALBERG, P. A. (2009). Critical review of the human data on short-term nitrogen dioxide (no<sub>2</sub>) exposures: Evidence for no<sub>2</sub>-effect levels. *Critical Reviews in Toxicology* **39**, 743–781.
- HOFFMAN, K. L., SALAZAR-BARRETO, D., WILLIAMS, N. T., RUDOLPH, K. E. & DÍAZ, I. (2024). Studying continuous, time-varying, and/or complex exposures using longitudinal modified treatment policies. *Epidemiology* **35**, 667–675.
- HOSHINO, T. & YANAGI, T. (2023). Causal inference with noncompliance and unknown interference. *Journal of the American Statistical Association*, 1–12.
- HUBBARD, A. E., KHERAD-PAJOUH, S. & VAN DER LAAN, M. J. (2016). Statistical inference for data adaptive target parameters. *The International Journal of Biostatistics* **12**, 3–19.
- HUDGENS, M. G. & HALLORAN, M. E. (2008). Toward causal inference with interference. *Journal of the American Statistical Association* **103**, 832–842.
- KENNEDY, E. H. (2022). Semiparametric doubly robust targeted double machine learning: A review. *arXiv:2203.06469*.
- KLAASSEN, C. A. J. (1987). Consistent estimation of the influence function of locally asymptotically linear estimators. *The Annals of Statistics*, 1548–1562.

- KOSHEVNIK, Y. A. & LEVIT, B. Y. (1977). On a non-parametric analogue of the information matrix. *Theory of Probability & Its Applications* **21**, 738–753.
- MORRISON, C. N., MAIR, C. F., BATES, L., DUNCAN, D. T., BRANAS, C. C., BUSHOVER, B. R., MEHRANBOD, C. A., GOBAUD, A. N., UONG, S., FORREST, S., ROBERTS, L. & RUNDLE, A. G. (2024). Defining spatial epidemiology: A systematic review and re-orientation. *Epidemiology* .
- OGBURN, E. L., SOFRYGIN, O., DÍAZ, I. & VAN DER LAAN, M. J. (2022). Causal inference for social network data. *Journal of the American Statistical Association* , 1–15.
- OHNISHI, Y., KARMAKAR, B. & SABBAGHI, A. (2022). Degree of interference: A general framework for causal inference under interference. *arXiv:2210.17516* .
- PEARL, J. (2000). Causality: Models, reasoning and inference. *Cambridge University Press* **19**, 3.
- PEARL, J. (2010). On the consistency rule in causal inference: Axiom, definition, assumption, or theorem? *Epidemiology* **21**, 872–875.
- PEBESMA, E. (2018). Simple Features for R: Standardized Support for Spatial Vector Data. *The R Journal* **10**, 439–446.
- PFANZAGL, J. & WEFELMEYER, W. (1985). Contributions to a general asymptotic statistical theory. *Statistics & Risk Modeling* **3**, 379–388.
- PHILLIPS, R. V., VAN DER LAAN, M. J., LEE, H. & GRUBER, S. (2023). Practical considerations for specifying a super learner. *International Journal of Epidemiology* **52**, 1276–1285.
- PRENER, CHRISTOPHER, REVORD & CHARLES (2019). areal: An R package for areal weighted interpolation. *Journal of Open Source Software* **4**.
- QIN, J. (1998). Inferences for case-control and semiparametric two-sample density ratio models. *Biometrika* **85**, 619–630.
- R CORE TEAM (2024). *R: A Language and Environment for Statistical Computing*. R Foundation for Statistical Computing, Vienna, Austria.
- REICH, B. J., YANG, S., GUAN, Y., GIFFIN, A. B., MILLER, M. J. & RAPPOLD, A. (2021). A review of spatial causal inference methods for environmental and epidemiological applications. *International Statistical Review* **89**, 605–634.
- ROBINS, J. M., HERNÁN, M. & SIEBERT, U. (2004). Effects of multiple interventions. In *Comparative Quantification of Health Risks: Global and Regional Burden of Disease Attributable to Selected Major Risk Factors*, M. Ezzati, A. D. Lopez, A. Rodgers & M. C. J. L, eds. World Health Organization.
- RUBIN, D. B. (1980). Randomization analysis of experimental data: The fisher randomization test comment. *Journal of the American Statistical Association* **75**, 591–593.
- RUBIN, D. B. (2005). Causal inference using potential outcomes: Design, modeling, decisions. *Journal of the American Statistical Association* **100**, 322–331.
- SHIN, H., BRAUN, D., IRENE, K., AUDIRAC, M. & ANTONELLI, J. (2023). A spatial interference approach to account for mobility in air pollution studies with multivariate continuous treatments. *arXiv:2305.14194* .
- SOFRYGIN, O. & VAN DER LAAN, M. J. (2017). Semi-parametric estimation and inference for the mean outcome of the single time-point intervention in a causally connected population. *Journal of causal inference* **5**, 20160003.
- SUGIYAMA, M., SUZUKI, T. & KANAMORI, T. (2012). *Density Ratio Estimation in Machine Learning*. Cambridge University Press.
- TCHETGEN TCHETGEN, E. J., FULCHER, I. R. & SHPITSER, I. (2021). Auto-g-computation of causal effects on a network. *Journal of the American Statistical Association* **116**, 833–844.
- TCHETGEN TCHETGEN, E. J. & VANDERWEELE, T. J. (2012). On causal inference in the presence of interference. *Statistical Methods in Medical Research* **21**, 55–75.
- UNITED STATES EPA (2018). National ambient air quality standards (NAAQS) for nitrogen dioxide.
- U.S. CENSUS BUREAU (2024). LEHD origin-destination employment statistics data (2002-2021). <https://lehd.ces.census.gov/data/#lodes>. Accessed: 2024-06-11.
- U.S. ENVIRONMENTAL PROTECTION AGENCY (2024). Smart location mapping. <https://www.epa.gov/smartgrowth/smart-location-mapping>. Accessed: 2024-06-10.
- VAN DER LAAN, M. J. (2014). Causal inference for a population of causally connected units. *Journal of causal inference* **2**, 13–74.

- VAN DER LAAN, M. J., DUDOIT, S. & KELES, S. (2004). Asymptotic optimality of likelihood-based cross-validation. *Statistical Applications in Genetics and Molecular Biology* **3**, 1–23.
- VAN DER LAAN, M. J., POLLEY, E. C. & HUBBARD, A. E. (2007). Super learner. *Statistical Applications in Genetics and Molecular Biology* **6**.
- VAN DER LAAN, M. J. & ROSE, S. (2011). *Targeted Learning: Causal Inference for Observational and Experimental Data*, vol. 4. Springer.
- VAN DER LAAN, M. J. & RUBIN, D. (2006). Targeted maximum likelihood learning. *The International Journal of Biostatistics* **2**.
- VAN DER VAART, A. W., DUDOIT, S. & VAN DER LAAN, M. J. (2006). Oracle inequalities for multi-fold cross validation. *Statistics & Decisions* **24**, 351–371.
- WALKER, K. & HERMAN, M. (2024). *tidycensus: Load US Census Boundary and Attribute Data as 'tidyverse' and 'sf'-Ready Data Frames*. R package version 1.6.3.
- YOUNG, J. G., HERNÁN, M. A. & ROBINS, J. M. (2014). Identification, estimation and approximation of risk under interventions that depend on the natural value of treatment using observational data. *Epidemiologic Methods* **3**, 1–19.
- ZHENG, W. & VAN DER LAAN, M. J. (2010). Asymptotic theory for cross-validated targeted maximum likelihood estimation. *bepress* .
- ZIGLER, C., LIU, V., MEALLI, F. & FORASTIERE, L. (2023). Bipartite interference and air pollution transport: Estimating health effects of power plant interventions. *arXiv:2012.04831* .
- ZIVICH, P. N., HUDGENS, M. G., BROOKHART, M. A., MOODY, J., WEBER, D. J. & AIELLO, A. E. (2022). Targeted maximum likelihood estimation of causal effects with interference: A simulation study. *Statistics in Medicine* **41**, 4554–4577.

---

# Supplementary Materials for

## THE CAUSAL EFFECTS OF MODIFIED TREATMENT POLICIES UNDER NETWORK INTERFERENCE

---

**Salvador V. Balkus**

Department of Biostatistics,  
Harvard T.H. Chan School of Public Health  
sbalkus@g.harvard.edu

**Scott W. Delaney**

Department of Environmental Health,  
Harvard T.H. Chan School of Public Health  
sdelaney@mail.harvard.edu

**Nima S. Hejazi<sup>†</sup>**

Department of Biostatistics,  
Harvard T.H. Chan School of Public Health  
nhejazi@hsph.harvard.edu

December 4, 2024

These supplementary materials provide proofs of the results presented in the main text, elaborations on some mathematical details, and extra figures and tables for the data analysis studying the effects of zero-emission vehicle uptake on NO<sub>2</sub> air pollution in California. Section S1 proves the identification result given in Section 3.2 of the main text. Section S2 proves Theorems 1 and 2 given in Section 3.3 describing the conditions under which an induced MTP is piecewise smooth invertible, and provides additional commentary on their mathematical implications. Section S3 proves that the one-step estimator given in Section 3.4 of the main text solves the EIF estimating equation, while Section S4 proves the consistency of its variance estimator. Finally, Section S5 provides additional summary statistics describing the data used in Section 5.

### S1 Identifying the causal effect of an induced MTP

Recall that the counterfactual mean under an induced MTP is given by the causal quantity  $\Psi_n(\mathbb{P}) = \mathbb{E}_{\mathbb{P}}\left(\frac{1}{n} \sum_{i=1}^n Y(h(a_i^s, l_i^s; \delta))\right)$ . Under the identifying assumptions given in the main text—positivity, no unmeasured confounding, and piecewise smooth invertibility of  $h$ —its identification proceeds as follows:

$$\begin{aligned}
 & \mathbb{E}_{\mathbb{P}}\left(\frac{1}{n} \sum_{i=1}^n Y(h(a_i^s, l_i^s; \delta))\right) && \text{(Definition)} \\
 &= \frac{1}{n} \sum_{i=1}^n \mathbb{E}_{\mathbb{P}}(Y(h(a_i^s, l_i^s; \delta))) && \text{(Linearity of expectation)} \\
 &= \frac{1}{n} \sum_{i=1}^n \mathbb{E}_{(L_i^s, A_i^s)}\left(\mathbb{E}_{\mathbb{P}}(Y_i \mid A_i^s = h(a_i^s, l_i^s; \delta), L_i^s = l_i^s)\right) && \text{(No unmeasured confounding, definition of NPSEM)} \\
 &= \frac{1}{n} \sum_{i=1}^n \int_{\mathcal{L}^s} \int_{\mathcal{A}^s} \mathbb{E}_{\mathbb{P}}(Y_i \mid A_i^s = h(a_i^s, l_i^s; \delta), L_i^s = l_i^s) p(a_i^s \mid l_i^s) p(l_i^s) \partial \mu(a_i^s, l_i^s) && \text{(Definition of expectation)} \\
 &= \frac{1}{n} \sum_{i=1}^n \int_{\mathcal{L}^s} \int_{\mathcal{A}^s} m(a_i^s, l_i^s) \cdot w(a_i^s, l_i^s) \cdot p(a_i^s \mid l_i^s) \cdot p(l_i^s) \partial \mu(a_i^s, l_i^s) \text{ where}
 \end{aligned}$$

$$w(a_i^s, l_i^s) := \sum_{k=1}^K \frac{p(h_k^{-1}(a_i^s, l_i^s) | l_i^s)}{p(a_i^s | l_i^s)} \cdot \frac{\partial h_k^{-1}(a_i^s, l_i^s)}{\partial a_i^s} \cdot \mathbb{I}(a_i^s \in \mathcal{A}_k^s)$$

(Change of variables  $h(a_i^s, l_i^s; \delta)$  for  $a_i^s$  via piecewise smooth invertibility)

Positivity is implicitly invoked from the third step onwards until the final step to guarantee that densities over which integration must be performed are well-defined. Note that for practical purposes, we rely on the implication of positivity that  $p(a_i^s | l_i^s)$  is bounded away from zero, which ensures that the ratio of densities in the fifth step is well-defined.

Technically, the above identification could be truncated at the third line, which is a statistical functional that does not rely on piecewise smooth invertibility (Assumption A3). However, as we discuss in the main text, semi-parametric efficiency theory necessitates an expression of the statistical functional in terms of its efficient influence function — which relies on both the conditional mean and density ratio — motivating identification to be performed in this way.

## S2 Form of the induced MTP function $h$

This section proves Theorems 1 and 2 from the main text. First, let us more formally define the mathematical context and notation used.

**Mathematical context:** In this work, we consider all  $n$ -length treatment vectors  $\mathbf{a}$  to be of finite dimension and in a Banach space with underlying field  $(\mathbb{R}^n, +, \cdot)$ , where  $+$  and  $\cdot$  are any operations satisfying the classical notion of a vector field and  $\mathbb{R}^n \subseteq \mathbb{R}^n$ . We also consider derivatives to be Fréchet. However, these Banach spaces are used simply to represent a vector space on which functions can have some minimal notion of differentiability; unfamiliar readers can assume the typical Euclidean  $\mathbb{R}^n$  vector space, though our proofs require no properties specific to it.

**Notation:** Recall from the main text that an induced MTP satisfies

$$h(s(\mathbf{a})) = s(d(\mathbf{a})) \tag{S1}$$

We assume that  $s(\mathbf{a})$  is a symmetric function (Assumption A4) mapping  $\mathbf{a}$  to another Banach space. For notational simplicity denote  $d(\mathbf{a}) = (d(x_1), \dots, d(x_n))$  where each component  $d(x_i)$  is piecewise smooth invertible in  $x_i$ ; hence,  $d(\mathbf{a})$  is the componentwise piecewise smooth invertible vector representation of  $d(x_i)$  for all  $i = 1, \dots, n$ .

**Overview of this section:** We first show the intermediate result that in order for  $h$  to be piecewise differentiable,  $s$  must be Lipschitz continuous (Section S2.1). The Lipschitz property implies that  $s$  is differentiable almost everywhere; its derivative is only undefined on a finite number of points in its domain. This provides a system of equations from which it is possible to solve for the derivative of  $h$  (Section S2.2). As a consequence, one can show that on each differentiable partition of its domain,  $s$  must be linear (Section S2.3), proving Theorem 1 which states that  $s$  must be a piecewise linear function. Finally, we prove Theorem 2 that if  $s$  is allowed to be any piecewise linear function, the only MTP function  $d$  that induces a piecewise differentiable  $h$  is  $d(\mathbf{a}) = \alpha \mathbf{a} + \beta$  (Section S2.4). We discuss the case where the treatment vector and network profile may be restricted in Section S2.5, and the implication of working on a Banach space in Section S2.6.

### S2.1 Proof: $s$ must be Lipschitz

In this section, we first prove an intermediate result useful in later proofs.

**Lemma S1.** *Suppose  $h(s(\mathbf{a})) = s(d(\mathbf{a}))$  for some piecewise differentiable  $d$ . If  $h$  is differentiable in  $s(\mathbf{a})$ , then  $s(\mathbf{a})$  must be Lipschitz, meaning that for any  $\mathbf{a}_1$  and  $\mathbf{a}_2$  in its domain,*

$$\|s(\mathbf{a}_1) - s(\mathbf{a}_2)\| \leq \gamma \|\mathbf{a}_1 - \mathbf{a}_2\| \tag{S2}$$

*holds for some constant  $\gamma$ .*

*Proof.* We proceed with a proof by contradiction. Assume that  $h$  is piecewise differentiable and that  $s$  is not Lipschitz.

First, we remind the reader of the differential definition of a derivative. Recall  $\Delta f(\mathbf{a}) = f(\mathbf{a} + \Delta \mathbf{a}) - f(\mathbf{a})$ . A function  $f$  is differentiable in  $\mathbf{a}$  if for some matrix  $A$  not depending on  $\Delta \mathbf{a}$ ,

$$\Delta f(\mathbf{a}) = A \Delta \mathbf{a} + O(\Delta \mathbf{a}) \tag{S3}$$

If  $h$  is piecewise differentiable in  $s(\mathbf{a})$ , then on any interval on which it is differentiable we can apply the definition of  $\Delta$  to write

$$\Delta h = A(\Delta s(\mathbf{a})) + O(\Delta s(\mathbf{a}))$$

$$= A(s(\mathbf{a} + \Delta\mathbf{a}) - s(\mathbf{a})) + O(s(\mathbf{a} + \Delta\mathbf{a}) - s(\mathbf{a}))$$

However, we can also rewrite  $\Delta h$  as

$$\begin{aligned} \Delta h &= h(s(\mathbf{a}) + \Delta s(\mathbf{a})) - h(s(\mathbf{a})) && \text{(Definition of } \Delta h) \\ &= h(s(\mathbf{a}) + s(\mathbf{a} + \Delta\mathbf{a}) - s(\mathbf{a})) - h(s(\mathbf{a})) && \text{(Definition of } \Delta s) \\ &= h(s(\mathbf{a} + \Delta\mathbf{a})) - h(s(\mathbf{a})) && \text{(Cancel } s(\mathbf{a}) \text{ terms)} \\ &= s(d(\mathbf{a} + \Delta\mathbf{a})) - s(d(\mathbf{a})) && \text{(Plug in Equation (S1))} \end{aligned}$$

yielding the equality

$$s(d(\mathbf{a} + \Delta\mathbf{a})) - s(d(\mathbf{a})) = A(s(\mathbf{a} + \Delta\mathbf{a}) - s(\mathbf{a})) + O(s(\mathbf{a} + \Delta\mathbf{a}) - s(\mathbf{a})) \quad (\text{S4})$$

If  $s$  is not Lipschitz (by assumption), then since  $d$  is differentiable on this domain, for some matrix  $D$ ,

$$\begin{aligned} \|s(d(\mathbf{a} + \Delta\mathbf{a})) - s(d(\mathbf{a}))\| &> \gamma \|d(\mathbf{a} + \Delta\mathbf{a}) - d(\mathbf{a})\| \\ &= \gamma \|D\Delta\mathbf{a} + O(\Delta\mathbf{a})\| \end{aligned}$$

But, plugging this inequality into Equation (S2.1), we have

$$\|A(s(\mathbf{a} + \Delta\mathbf{a}) - s(\mathbf{a})) + O(s(\mathbf{a} + \Delta\mathbf{a}) - s(\mathbf{a}))\| > \gamma \|D\Delta\mathbf{a} + O(\Delta\mathbf{a})\| \quad (\text{S5})$$

which is clearly not true for  $\Delta\mathbf{a} = \mathbf{0}$ , since this would imply  $0 > 0$ . Since this contradiction arises, if  $h$  is differentiable in  $s(\mathbf{a})$ , it must be true that  $s$  is Lipschitz.  $\square$

## S2.2 The implication of $s$ being Lipschitz

Lemma S1 states that if  $h$  is piecewise differentiable, then  $s$  is Lipschitz. This implies  $s$  is continuously differentiable almost everywhere, meaning its domain can be partitioned into a finite number of subsets such that on each partition,  $s$  is continuously differentiable. Denote the derivative of a function  $f(\mathbf{a})$  with respect to  $\mathbf{a}$  – the Jacobian matrix function for  $f$  with domain  $\mathbb{R}^n$  – as  $J_f$ .

Since  $h(s(\mathbf{a})) = s(d(\mathbf{a}))$  by definition, it must be possible to differentiate both sides of this equation with respect to  $\mathbf{a}$ . Differentiating both sides by applying the chain rule, we have

$$J_h(s(\mathbf{a}))J_s(\mathbf{a}) = J_s(d(\mathbf{a}))J_d(\mathbf{a}) \quad (\text{S6})$$

which must hold on each ‘‘piece’’ of the piecewise continuous derivative  $J_h$  of  $h$ . That is,  $J_h(s(\mathbf{a}))$  is the quantity that needs to exist on any given partition of  $\mathcal{A}$  for  $h$  to be piecewise differentiable. Computing the derivative of  $h$  amounts to solving this equation for  $J_h(s(\mathbf{a}))$  – a fact that we use in subsequent sections.

## S2.3 Proof of Theorem 1: if $h$ is piecewise differentiable, then $s$ must be piecewise linear

Theorem 1 states that if  $h$  is piecewise differentiable, then  $s$  must be piecewise linear. Here, we prove that  $s$  cannot be nonlinear; this, combined with the proof in Section S2.4 that linearity is sufficient to induce a piecewise smooth  $h$ , proves that  $s$  must be linear. The proof follows from Equation (S6) in Section S2.2.

*Proof.* Assume  $h$  is piecewise continuously differentiable, and that  $s$  is nonlinear. Recall that if  $h$  is continuously differentiable on a partition of  $\mathcal{A}$ , it must satisfy Equation (S6). Therefore,

$$J_s^\top(\mathbf{a})J_h^\top(s(\mathbf{a})) = (J_s(d(\mathbf{a}))J_d(\mathbf{a}))^\top \quad (\text{S7})$$

must be solvable for  $J_h^\top(s(\mathbf{a}))$  for all  $\mathbf{a} \in \mathcal{A}_k \subset \mathcal{A}$ . It is not possible to cancel the summary function Jacobians unless  $J_s(\mathbf{a}) = J_s(d(\mathbf{a}))$  for all  $\mathbf{a} \in \mathcal{A}_k$ , which only occurs if  $s$  is linear and therefore is known not to be true. Therefore, this system cannot be solved by ‘‘undoing’’ the right-multiplication of  $J_s$ ; it can only be solved via Gaussian elimination.

A fundamental result in linear algebra tells us that for a system of matrix equations to be solvable for some *arbitrary* unknown, the matrix of coefficients must be invertible (Gentle, 2007). Unfortunately,  $J_s(\mathbf{a})$  must always be singular, and therefore not invertible, under some choice of network profile and covariates. Why is this? Under Assumption A4 that  $s$  is symmetric, if entry  $i$  of  $s(\mathbf{a})$  depends on at least two units  $j$  and  $k$  (with  $j \neq k$ ), then each entry of the  $i$  row of  $J_s(\mathbf{a})$  must be the same function of  $\mathbf{a}$ . If they were different functions, entries of  $s$  would not be symmetric under

permutation of their arguments. Consequently, we can always choose a network profile and set of covariates so that  $J_s(\mathbf{a})$  contains two rows that can be row-reduced into rows of zeros.

As an example, suppose the network profile contained a subgraph of two units connected only to each other, and their outcome under interference depends on a sum of some function of their treatments; that is,  $s(\mathbf{a})_i = \sum_{j \in F_i} f(x_j)$ . Then, the Jacobian  $J_s(\mathbf{a})$  would contain the block

$$\begin{bmatrix} \frac{\partial}{\partial a_1} f(a_1) & \frac{\partial}{\partial a_2} f(a_2) \\ \frac{\partial}{\partial a_1} f(a_1) & \frac{\partial}{\partial a_2} f(a_2) \end{bmatrix} \quad (\text{S8})$$

Clearly,  $J_s(\mathbf{a})$  is singular as row 1 and row 2 can be subtracted to create a row of all zeros.

Consequently, since  $J_s$  may always be singular, there is no guarantee  $J_s$  is invertible for an arbitrary network profile. Since no solution for  $J_h^\top(s(\mathbf{a}))$  may exist, this contradicts our original statement that  $h$  must be differentiable. Therefore, if  $s$  is nonlinear,  $h$  cannot be differentiated (unless further restrictions are imposed; see Section S2.5). By the contrapositive, if  $h$  is differentiable on a partition  $\mathcal{A}_k$  of  $\mathcal{A}$ ,  $s$  must be linear; combining its derivative on each partition on which  $s$  is differentiable,  $s$  must be piecewise linear.  $\square$

### S2.4 Proof of Theorem 2: The form of $d$ when $s$ is linear

In this section, we prove that if  $s$  is linear, then  $d(\mathbf{a}) = \alpha \mathbf{a} + \beta$  where  $\alpha$  is a constant scalar and  $\beta$  is a vector such that  $\frac{\partial}{\partial \mathbf{a}} \beta = 0$ . Intuitively, what this means is that if the interference takes the form of a linear combination of neighbors, then the only MTP interventions whose causal effects are identified for all such  $s$  are (a) adding some constant  $\beta_i$  (that may depend on covariates) to the treatment of unit  $i$ , or (b) scaling all units' treatments by some value  $\alpha$  (or both (a) and (b) at once).

*Proof.* If  $s$  is linear on some partition of  $\mathcal{A}$ , its derivative is the constant matrix  $S$  for all  $\mathbf{a}$ . Plugging this into Equation (S6), we get

$$J_h(S\mathbf{a})S = SJ_d(\mathbf{a}) \quad (\text{S9})$$

Recall that for a system of matrix equations to be solvable for some arbitrary unknown without further assumptions, the matrix of coefficients must be invertible (Gentle, 2007). Again, note that since each entry of  $s(\mathbf{a})$  is a symmetric function of  $\mathbf{a}$ , each entry of  $S$  must be identical. If they were not, then this would imply  $s(\mathbf{a})$  depends differently on different entries of  $\mathbf{a}$  and therefore a given entry of  $s(\mathbf{a})$  would not be identical under permutation. This implies  $S$  is singular by definition (except in the trivial case where each unit depends only on itself, in which case there is no interference) and therefore  $S$  is not invertible.

As an example, suppose the network profile contained a subgraph of two units connected only to each other, and their outcome under interference depends on a *weighted sum* of neighboring treatments; that is,  $s(\mathbf{a})_i = \sum_{j \in F_i} w_j x_j$ . Then, the Jacobian  $S$  would contain the block

$$\begin{bmatrix} w_1 & w_2 \\ w_1 & w_2 \end{bmatrix} \quad (\text{S10})$$

which is clearly singular since it can be row-reduced into two rows of all zeros. Therefore, the only way to solve this system is to exploit the fact that if  $J_d(\mathbf{a})$  could commute with  $S$ , then  $S$  could be canceled from both sides. But the only type of matrix that can commute with any arbitrary  $n \times n$  matrix is a scalar matrix – one of the form  $\alpha I$  where  $\alpha$  is a constant scalar. As a result, for this system to be solvable for  $J_h$ , it must be that  $J_d(\mathbf{a}) = \alpha I$ . Note that  $J_d$  is already assumed to be diagonal since each  $i^{\text{th}}$  entry  $d(x_i)$  depends only on  $x_i$ , the  $i^{\text{th}}$  entry of  $\mathbf{a}$ , so this is a valid form of  $J_d(\mathbf{a})$ .

Since each entry of the diagonal of  $J_d$  is the derivative of the corresponding  $d(\mathbf{a})$  entry, if  $J_d$  is a constant scalar diagonal then each  $d(a_i)$  must be linear. This implies  $d(\mathbf{a}) = \alpha \mathbf{a} + \beta$  where the derivative of  $\beta$  is 0, proving the desired result.

Note that this condition still permits piecewise MTPs—such as that given in Equation (3)—that apply a different additive shift depending on indicator functions of  $a_i$ . Piecewise summaries of  $K$  pieces  $s_1, \dots, s_K$  take the form

$$s(\mathbf{a}) = \sum_{k=1}^K s_k(\mathbf{a}) \mathbb{I}(\mathbf{a} \in \mathcal{A}_k^s) \quad (\text{S11})$$

Simply let each entry of  $\beta$  depend on an indicator function of  $A_i$ ; then, its derivative with respect to  $\mathbf{a}$  and  $s(\mathbf{a})$  is zero, and we have by piecewise linearity

$$\begin{aligned} \frac{\partial}{\partial s(\mathbf{a})} h(s(\mathbf{a}))^{-1} &= \frac{\partial}{\partial s(\mathbf{a})} \left( \sum_{k=1}^K s_k(\alpha \mathbf{a} + \beta) \mathbb{I}(\alpha \mathbf{a} + \beta \in \mathcal{A}_k^s) \right)^{-1} \\ &= \frac{\partial}{\partial s(\mathbf{a})} \left( \alpha \sum_{k=1}^K s_k(\mathbf{a}) \mathbb{I}(\alpha \mathbf{a} + \beta \in \mathcal{A}_k^s) + \sum_{k=1}^K s_k(\beta) \mathbb{I}(\alpha \mathbf{a} + \beta \in \mathcal{A}_k^s) \right)^{-1} \\ &= 1/\alpha \end{aligned}$$

□

## S2.5 A remark on other possible forms of $J_s(\mathbf{a})$

So far, we have laid out conditions for  $h$  to be differentiable for all possible network profiles  $\mathbf{F}$  and random vectors  $\mathbf{a}$ . However, it may be possible to place other restrictions on  $\mathbf{a}$  and  $\mathbf{F}$ . While we cannot consider every possible further restriction one could postulate, there are two interesting cases in which relatively mild restrictions could guarantee  $h$  is differentiable.

First, assume that  $\mathbf{F}$  is the adjacency matrix of a directed graph with no cycles. In this case, the rows of  $\mathbf{F}$  can be permuted into a triangular matrix, which implies that  $J_s(\mathbf{a})$  can be made triangular (which is not necessarily true if  $\mathbf{F}$  is undirected or contains cycles). Assumption A5 guarantees the diagonal entries of this matrix are nonzero; therefore, this restriction guarantees  $J_s(\mathbf{a})$  nonsingular. Then, we can solve Equation S6 for  $J_h$  through Gaussian elimination. A similar result can be accomplished if the summary happens to ensure  $J_s(\mathbf{a})$  is triangular regardless of  $\mathbf{F}$  (i.e. by being dependent on covariate values).

Second, if  $s$  is linear and  $J_s$  happens to be a symmetric matrix – for instance, an unweighted sum over a random graph with undirected edges – then since  $J_d(\mathbf{a})$  is diagonal, it always commutes with  $J_s(\mathbf{a})$ , even if the individual entries of  $d(\mathbf{a})$  are not linear functions. As a result, it follows from Equation S9 that  $J_d(\mathbf{a}) = J_h(\mathbf{a})$ .

That said, these are relatively specific use cases, since the definition of  $s$  and  $\mathbf{F}$  typically follow from the scientific problem at hand and cannot be chosen arbitrarily. The first also requires numerical routines to solve for  $h$ , since it admits no closed-form analytical solution. Even if  $J_s(\mathbf{a})$  is theoretically nonsingular, there is no guarantee that it is sufficiently well-conditioned for the system to be solved numerically. Hence, we reserve our theory to piecewise linear summaries, the only forms of  $s$  that guarantee  $J_h$  exists under no further restriction.

## S2.6 The implication of the vector space on the form of summary

An important point to emphasize regarding Sections S2.1-S2.4 is that all mathematical reasoning is conducted only with respect  $\mathbf{a}$  in an arbitrary Banach space, with functions that also map to Banach spaces. Recall the previous statement that elements of these spaces are in a vector field  $(\mathbb{R}^n, +, \cdot)$ . The operators  $+$ ,  $\cdot$  can be arbitrary, as long as they satisfy the definition of a vector field.

As such, the class of functions  $s$  and  $d$  that qualify as “linear” for the purposes of an aggregator are much larger than they might appear at first glance. For example, if  $\mathbb{R}^n$  is restricted to positive real vectors, the geometric mean

$$s(\mathbf{a}) = \left[ \left( \prod_{j \in F_i} a_j \right)^{1/|F_i|} \right]_{i=1}^n \quad (\text{S12})$$

is linear, as is the highly flexible MTP function  $d(a_i, l_i; \delta) = x_i^\delta \cdot q(l_i, \delta)$  for some arbitrary function  $q(l_i, \delta) \in \mathbb{R}^+$ . These functions are linear on the vector space where the  $+$  operator is equivalent to our traditional notion of multiplication, and the  $\cdot$  operator is equivalent to our traditional notion of raising to a power.

Since the previous proofs hold for all Banach spaces as we defined them, they are agnostic to the actual binary operators within the vector field of that Banach space. So, as long as  $s$  and  $d$  are both linear with respect to the vector field’s binary operations, or  $d$  maps to a new vector field with binary operations on which  $s$  is still linear (such as log transform mapping multiplication to addition), then our previous proofs will hold. In this way, a broad class of linear  $d$  and  $s$  can be constructed, beyond the restrictive traditional definitions of  $+$  and  $\cdot$  that might be assumed in a Euclidean vector space.

### S3 One-step estimator

Here, we prove that the one-step estimator given by Equation (12) in the main text solves the EIF estimating equation asymptotically and is therefore consistent and semi-parametric efficient.

*Proof.* Solving the EIF in Equation (10) directly for  $\psi_n$  yields the quantity

$$\psi_n = \frac{1}{n} \sum_{i=1}^n \hat{w}(A_i^s, L_i^s)(Y_i - \hat{m}(A_i^s, L_i^s)) + \mathbb{E}_P(\hat{m}(h(A_i^s, L_i^s; \delta), L_i^s) \mid \mathbf{L} = \mathbf{1}) \quad (\text{S13})$$

Distributing the summation linearly, this can be divided into two components, which both converge asymptotically by Theorem 3:

$$\begin{aligned} & \frac{1}{n} \sum_{i=1}^n \hat{w}(A_i^s, L_i^s)(Y_i - \hat{m}(A_i^s, L_i^s)) \xrightarrow{P} \mathbb{E}_P(\hat{w}(A_i^s, L_i^s)(Y_i - \hat{m}(A_i^s, L_i^s))) \\ & \frac{1}{n} \sum_{i=1}^n \mathbb{E}_{\mathbf{A}|\mathbf{L}}(\hat{m}(h(A_i^s, L_i^s; \delta), L_i^s) \mid \mathbf{L} = \mathbf{1}) \xrightarrow{P} \mathbb{E}_{\mathbf{L}}(\mathbb{E}_{\mathbf{A}|\mathbf{L}}(\hat{m}(h(A_i^s, L_i^s; \delta), L_i^s) \mid \mathbf{L} = \mathbf{1})) \\ & = \mathbb{E}_{\mathbf{L}, \mathbf{A}}(\hat{m}(h(A_i^s, L_i^s; \delta))), \end{aligned}$$

where the third line follows from the law of total expectation. The second component is the plug-in estimate, and the first component corrects the bias of the plug-in estimate. But, recall that equivalently, the direct plug-in estimator also converges (assuming  $\hat{m}$  is consistent):

$$\frac{1}{n} \sum_{i=1}^n \hat{m}(h(A_i^s, L_i^s; \delta)) \xrightarrow{P} \mathbb{E}_{\mathbf{L}, \mathbf{A}}(\hat{m}(h(A_i^s, L_i^s; \delta), L_i^s)) \quad (\text{S14})$$

Therefore, by the continuous mapping theorem,

$$\begin{aligned} \hat{\psi}_n^{\text{OS}} &= \frac{1}{n} \sum_{i=1}^n \hat{w}(a_i^s, l_i^s)(Y_i - \hat{m}(A_i^s, L_i^s)) + \frac{1}{n} \sum_{i=1}^n \hat{m}(h(A_i^s, L_i^s; \delta), L_i^s) \\ &\xrightarrow{P} \mathbb{E}_P(\hat{w}(A_i^s, L_i^s)(Y_i - \hat{m}(A_i^s, L_i^s))) + \mathbb{E}_{\mathbf{L}, \mathbf{A}}(\hat{m}(h(A_i^s, L_i^s; \delta))) = \psi_n \end{aligned}$$

proving that the one-step solves the same estimating equation as Equation (9) asymptotically.  $\square$

### S4 Variance estimator

In this section we prove that  $\hat{\sigma}^2$  as defined in Section 3.6 is a consistent estimator of the variance of  $\hat{\psi}_n^{\text{OS}}$ , and by extension, the variance of  $\hat{\psi}_n^{\text{TMLE}}$ .

#### S4.1 Consistency of $\hat{\psi}(|F_i|)$

First, we prove that  $\hat{\psi}(|F_i|)$  is consistent for its mean; specifically, we show  $\hat{\psi}(|F_i|) - E(\phi_{\hat{P}_n}(O_i)) = o_P(n^{-1/4})$ , which provides a rate that we can plug in algebraically in a later proof. In Section 3.2 we assumed that  $P(A_i^s) > 0$  for all  $i$ . For this assumption to hold true, the number of friends of any unit  $i$  cannot grow asymptotically slower than any other unit  $j$ . Formally, this means  $|\mathcal{N}(|F_i|)| \propto |\mathcal{N}(|F_j|)|$  for all  $i, j \in 1, \dots, n$ .

Next, recall that convergence of the one-step estimator assumes that the maximum degree of any node in the network encoded by  $\mathbf{F}$  grows no faster than  $n^{1/2}$ . More formally, this means  $\max_i |F_i| = O(n^{1/2})$ . Since  $|\mathcal{N}(|F_i|)| \propto |\mathcal{N}(|F_j|)|$ , for all  $i, j$ , noting that  $n/n^{1/2} = n^{1/2}$ , it must be true that  $|\mathcal{N}(|F_i|)| = O(n^{1/2})$  for all  $i$ . Then, recalling that  $\hat{\psi}_n^{\text{OS}} - \psi_n = o_P(n^{-1/2})$  for networks of bounded degree, computing the one-step estimator on the subset of nodes  $\mathcal{N}(|F_i|)$  (which have identical and therefore bounded degree) yields

$$\hat{\psi}_n(|F_i|) - E(\phi_{\hat{P}_n}(O_i)) = o_P(|\mathcal{N}(|F_i|)|^{-1/2}) = o_P(O(n^{1/2})^{-1/2}) = o_P(n^{-1/4}) \quad (\text{S15})$$

This completes the proof that the one-step estimator  $\hat{\psi}(|F_i|)$  converges to  $E(\phi_{\hat{P}_n}(O_i))$ , specifically at rate  $o_P(n^{-1/4})$ .

#### S4.2 Bias and variance of estimating function

Next, we prove that the estimating function  $\phi_{\hat{P}_n}(O_i) - \hat{\psi}_n(|F_i|)$  is unbiased, and that its variance is equal to that of the one-step estimator. First, note that under the assumed NPSEM in Section 3.2,  $\phi_{\hat{P}_n}(O_i)$  and  $\phi_{\hat{P}_n}(O_j)$  are identically distributed if  $|F_i| = |F_j|$ . Consequently,

$$\mathbb{E}(\phi_{\hat{P}_n}(O_i) - \hat{\psi}_n(|F_i|)) = \mathbb{E}(\phi_{\hat{P}_n}(O_i)) - \frac{1}{\mathcal{N}(|F_i|)} \sum_{j \in \mathcal{N}(|F_i|)} \mathbb{E}(\phi_{\hat{P}_n}(O_j)) = \mathbb{E}(\phi_{\hat{P}_n}(O_i)) - \mathbb{E}(\phi_{\hat{P}_n}(O_j)) \quad (\text{S16})$$

Since  $|F_i| = |F_j|$  by definition of  $\mathcal{N}(|F_i|)$ ,  $\mathbb{E}(\phi_{\hat{P}_n}(O_i)) - \mathbb{E}(\phi_{\hat{P}_n}(O_j)) = 0$ . Secondly, by variance properties, the variance of our one-step estimating equation can be rewritten as follows:

$$\begin{aligned} \text{Var}\left(\frac{1}{n} \sum_{i=1}^n \phi_{\hat{P}_n}(O_i) - \psi\right) &= \frac{1}{n^2} \sum_{i,j} \mathbb{E}\left((\phi_{\hat{P}_n}(O_i) - \mathbb{E}(\phi_{\hat{P}_n}(O_i)))(\phi_{\hat{P}_n}(O_j) - \mathbb{E}(\phi_{\hat{P}_n}(O_j)))\right) \\ &= \text{Var}\left(\frac{1}{n} \sum_{i=1}^n (\phi_{\hat{P}_n}(O_i) - \mathbb{E}(\phi_{\hat{P}_n}(O_i)))\right) = \sigma^2 \end{aligned}$$

the variance of  $\hat{\psi}_n^{\text{OS}}$  that we want to estimate, which completes the proof.

#### S4.3 Proof of plug-in variance consistency

Finally, we prove that the plug-in variance estimator converges to  $\sigma^2$ . This variance estimator is

$$\hat{\sigma}^2 = \frac{1}{n^2} \sum_{i,j} G(i,j) \varphi_i \varphi_j \quad (\text{S17})$$

where  $\varphi_i = \phi_{\hat{P}_n}(O_i) - \hat{\psi}_n(|F_i|)$ . By adding and subtracting to obtain the equality

$$\phi_{\hat{P}_n}(O_i) - \hat{\psi}_n(|F_i|) = \phi_{\hat{P}_n}(O_i) - E(\phi_{\hat{P}_n}(O_i)) + E(\phi_{\hat{P}_n}(O_i)) - \hat{\psi}_n(|F_i|)$$

we can decompose this estimator as follows:

$$\begin{aligned} \hat{\sigma}^2 &= \frac{1}{n^2} \sum_{i,j} G(i,j) (\phi_{\hat{P}_n}(O_i) - \hat{\psi}_n(|F_i|)) (\phi_{\hat{P}_n}(O_j) - \hat{\psi}_n(|F_j|)) \\ &= \frac{1}{n^2} \sum_{i,j} G(i,j) (\phi_{\hat{P}_n}(O_i) - E(\phi_{\hat{P}_n}(O_i))) (\phi_{\hat{P}_n}(O_j) - E(\phi_{\hat{P}_n}(O_j))) \\ &\quad - \frac{1}{n^2} \sum_{i,j} G(i,j) (\phi_{\hat{P}_n}(O_i) - E(\phi_{\hat{P}_n}(O_i))) (\hat{\psi}_n(|F_j|) - E(\phi_{\hat{P}_n}(O_j))) \\ &\quad - \frac{1}{n^2} \sum_{i,j} G(i,j) (\phi_{\hat{P}_n}(O_j) - E(\phi_{\hat{P}_n}(O_j))) (\hat{\psi}_n(|F_i|) - E(\phi_{\hat{P}_n}(O_i))) \\ &\quad + \frac{1}{n^2} \sum_{i,j} G(i,j) (\hat{\psi}_n(|F_i|) - E(\phi_{\hat{P}_n}(O_i))) (\hat{\psi}_n(|F_j|) - E(\phi_{\hat{P}_n}(O_j))) \end{aligned} \quad (\text{S18})$$

From Ogburn et al. (2022), we know

$$\frac{1}{n^2} \sum_{i,j} G(i,j) (\phi_{\hat{P}_n}(O_i) - E(\phi_{\hat{P}_n}(O_i))) (\phi_{\hat{P}_n}(O_j) - E(\phi_{\hat{P}_n}(O_j))) \xrightarrow{P} \sigma^2 \quad (\text{S19})$$

Furthermore, we know that the one-step estimator is  $\sqrt{C_n}$ -consistent, and since in Section S4.1 we proved that  $\hat{\psi}_n(|F_j|) - E(\phi_{\hat{P}_n}(O_j)) = o_P(n^{-1/4})$ , by the continuous mapping theorem,

$$\begin{aligned} &\frac{1}{n^2} \sum_{i,j} G(i,j) (\phi_{\hat{P}_n}(O_i) - E(\phi_{\hat{P}_n}(O_i))) (\hat{\psi}_n(|F_j|) - E(\phi_{\hat{P}_n}(O_j))) \\ &= \left(\frac{1}{n} \sum_i (\phi_{\hat{P}_n}(O_i) - E(\phi_{\hat{P}_n}(O_i)))\right) \left(\frac{1}{n} \sum_j (\hat{\psi}_n(|F_j|) - E(\phi_{\hat{P}_n}(O_j)))\right) \end{aligned} \quad (\text{S20})$$

$$= o_P(C_n^{-1/2}) \cdot o_P(n^{-1/4}) = o_P(C_n^{-1/2} \cdot n^{-1/4})$$

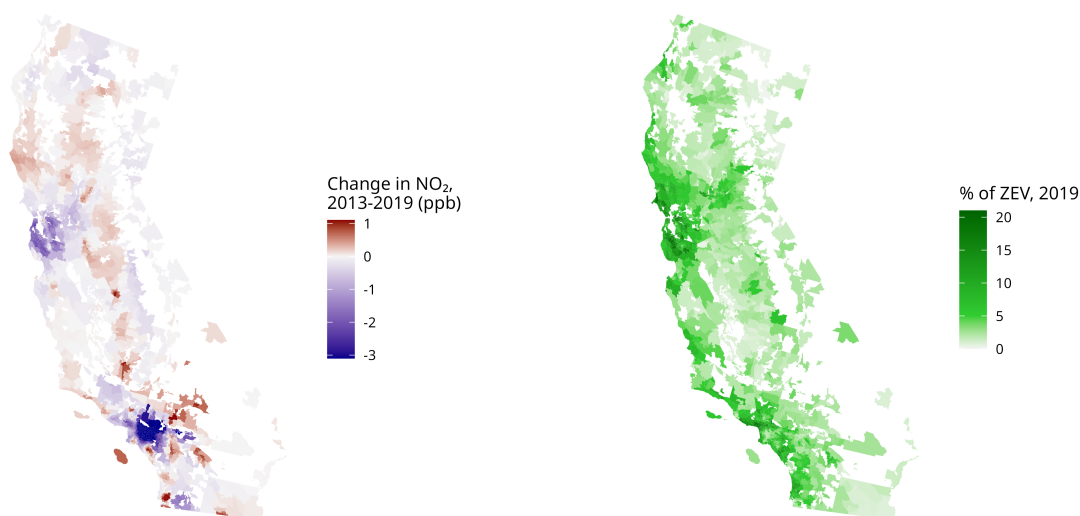
and also

$$\begin{aligned} & \frac{1}{n^2} \sum_{i,j} G(i,j) (\hat{\psi}_n(|F_i|) - E(\phi_{\hat{P}_n}(O_i))) (\hat{\psi}_n(|F_j|) - E(\phi_{\hat{P}_n}(O_j))) \\ &= \left( \frac{1}{n} \sum_i (\hat{\psi}_n(|F_i|) - E(\phi_{\hat{P}_n}(O_i))) \right) \left( \frac{1}{n} \sum_j (\hat{\psi}_n(|F_j|) - E(\phi_{\hat{P}_n}(O_j))) \right) \quad (\text{S21}) \\ &= o_P(n^{-1/4}) \cdot o_P(n^{-1/4}) = o_P(n^{-1/2}), \end{aligned}$$

implying that the second, third, and fourth terms in Equation (S18) converge to 0. Since the first term converges in probability to  $\sigma^2$ , we have thereby proven that  $\hat{\sigma}^2 \xrightarrow{P} \sigma^2$ .

## S5 Data Analysis

In this final section, we include extra summary statistics for the dataset used to analyze the effect of zero-emission vehicle uptake on  $\text{NO}_2$  air pollution in California. Figure S1 depicts the spatial distribution of the treatment and outcome across the study region of California. Table 1 displays basic summary statistics for the treatment (Change in  $\text{NO}_2$ , 2013-2019), outcome (Percentage of ZEVs, 2019), and confounders controlled in the analysis.



(a)  $\text{NO}_2$  air pollution in California.

(b) ZEV prevalence in California.

Figure S1: Spatial distribution of outcome ( $\text{NO}_2$ ) and treatment (ZEV) variables in the data example.

Table 1: Summary statistics of ZEV-NO<sub>2</sub> data, including confounders ( $n = 1652$ )

Statistic	Mean	Median	25 <sup>th</sup> pctl.	75 <sup>th</sup> pctl.
Change in NO <sub>2</sub> , 2013-2019 (ppb)	-0.6	-0.1	-0.9	0.1
% ZEV (of registered vehicles) , 2019	5.4	4.2	2.3	7.6
% ZEV (of registered vehicles), 2013	2.7	2.0	1.1	3.6
Population	23,753	19,505	2,485	38,478
Median income (\$)	76,944	69,156	51,299	95,552
Median home value (\$)	551,847	448,650	277,150	704,850
Median age (years)	40.9	39.2	34.4	46.1
% pop. college educated	32.3	27.7	16.3	46.2
% pop. high school educated	84.7	89.0	78.6	94.4
% pop. white	69.4	73.7	55.7	85.8
% pop. in poverty	10.1	7.5	3.8	14.1
% of homes owner-occupied	59.8	62.6	47.6	74.1
% pop. who take automobile to work	72.8	76.2	69.5	80.2
% pop. who take public transit to work	3.5	1.2	0.0	3.5
% pop. who work from home	8.0	6.0	3.8	9.7
Industrial employment (jobs/acre)	0.6	0.1	0.01	0.5
Road density (per acre)	11.1	6.8	2.4	19.8
Public transit frequency (peak, per hour)	5.4	1.0	0.1	4.9
Walkability index	8.7	7.6	5.1	12.3
Network degree	505.4	594	227.5	742

## References

- GENTLE, J. E. (2007). Matrix algebra. *Springer texts in statistics*, Springer, New York, NY, doi **10**, 978–0.
- OGBURN, E. L., SOFRYGIN, O., DÍAZ, I. & VAN DER LAAN, M. J. (2022). Causal inference for social network data. *Journal of the American Statistical Association* , 1–15.